Atmos. Chem. Phys. Discuss., 13, 6971–7019, 2013
www.atmos-chem-phys-discuss.net/13/6971/2013/
doi:10.5194/acpd-13-6971-2013

Atmospheric
Chemistry
and Physics
Discussions
Open Access

Variability of carbonaceous aerosols in remote, rural, urban and industrial environments in Spain: implications for air quality policy

X. Querol[1], A. Alastuey[1], M. Viana[1], T. Moreno[1], C. Reche[1], M.C. Minguillón[1], A. Ripoll[1], M. Pandolfi[1], F. Amato[1], A. Karanasiou[1], N. Pérez[1], J. Pey[1], M. Cusack[1], R. Vázquez[1], F. Plana[1], M. Dall'Osto[1], J. de la Rosa[2], A. de la Campa Sánchez[2], R. Fernández-Camacho[2], S. Rodríguez[3], C. Pío[4], L. Alados-Arboledas[5], G. Titos[5], B. Artíñano[6], P. Salvador[6], S. Dos Santos García[7], and R. Patier Fernández[7]

[1]Institute of Environmental Assessment and Water Research, IDAEA, CSIC, Barcelona, Spain
[2]Associate Unit CSIC – University of Huelva "Atmospheric Pollution", Center for Research in Sustainable Chemistry (CIQSO), University of Huelva, Huelva, Spain
[3]Centro de Investigación Atmosférica de Izaña (CIAI) de AEMET, Santa Cruz de Tenerife, Spain
[4]CESAM & Department of Environment, University of Aveiro, Portugal
[5]Departamento de Física Aplicada, Universidad de Granada, Spain

Title Page
Abstract | Introduction
Conclusions | References
Tables | Figures
I◀ | ▶I
◀ | ▶
Back | Close
Full Screen / Esc
Printer-friendly Version
Interactive Discussion

[6]CIEMAT, Madrid, Spain
[7]Instituto de Salud Carlos III, Madrid, Spain

Received: 19 December 2012 – Accepted: 22 February 2013 – Published: 15 March 2013

Correspondence to: X. Querol (xavier.querol@idaea.csic.es)

Published by Copernicus Publications on behalf of the European Geosciences Union.

Abstract

We interpret here the variability of levels of carbonaceous aerosols based on a 12-yr database from 78 monitoring stations across Spain especially compiled for this article. Data did not evidence any spatial trends of carbonaceous aerosols across the country. Conversely, results show marked differences in average concentrations from the cleanest, most remote sites (around 1 µg m^{-3} of non-mineral carbon (nmC), mostly made of organic carbon (OC), with very little elemental carbon (EC) 0.1 µg m^{-3}; OC/EC = 12–15), to the highly polluted major cities (8–10 µg m^{-3} of nmC; 3–4 µg m^{-3} of EC; 4–5 µg m^{-3} of OC; OC/EC = 1–2). Thus, urban (and very specific industrial) pollution was found to markedly increase levels of carbonaceous aerosols in Spain, with much lower impact of biomass burning.

Correlations between yearly averaged OC/EC and EC concentrations adjust very well to a potential equation ($\text{OC/EC} = 3.37\ \text{EC}^{-0.67}$ $R^2 = 0.94$). A similar equation is obtained when including average concentrations obtained at other European sites ($y = 3.61x^{-0.5}$, $R^2 = 0.78$).

A clear seasonal variability in OC and EC concentrations was detected. Both OC and EC concentrations were higher during winter at the traffic and urban sites, but OC increased during the warmer months at the rural sites. Hourly equivalent black carbon (EBC) concentrations at urban sites accurately depict road traffic contributions, varying with distance to road, traffic volume and density, mixing layer height and wind speed. Weekday urban rush-hour EBC peaks are mimicked by concentrations of primary gaseous emissions from road traffic, whereas a single midday peak is characteristic of remote and rural sites. Decreasing annual trends for carbonaceous aerosols were observed between 1999 and 2011 at a large number of stations, probably reflecting the impact of the EURO4 and EURO5 standards in reducing the diesel PM emissions. This has resulted in some cases in an increasing trend of NO_2/OC+EC ratios, because these standards have been much less effective for the abatement of NO_x exhaust emissions in passenger diesel cars. This study concludes that EC, EBC, and

especially nmC and OC+EC are very good candidates for new air quality standards since they cover both emission impact and health related issues.

1 Introduction

Carbonaceous material accounts for typically 10 to 50 % of the total particulate matter (PM_{10}) mass concentration (Putaud et al., 2010). Particulate carbon may be classified into three components: organic carbon (OC), elemental carbon (EC, sometimes used as an equivalent to black carbon, BC) and carbonate or mineral carbon (CC). The term non mineral carbon (nmC) is used for the concentrations of total carbon once CC has been subtracted. OC can be of both primary and secondary origin, i.e. emitted directly into the atmosphere or formed by the condensation of compounds produced in the atmosphere by photo-oxidation of volatile organic precursors (Fuzzi et al., 2006). In contrast, EC is exclusively of primary origin (incomplete combustion of carbon containing fuels, and to a lesser extent brake wear). CC is another primary carbonaceous species and is present in natural ground and building/construction dust.

Most of the carbonaceous PM present in the atmosphere arises from fuel combustion (fossil or not). Industrial processes and biogenic emissions may also account for a large proportion of the carbonaceous aerosol mass (both primary and secondary) depending on the monitored environment (Jimenez et al., 2009). Soil and road/urban dust particles may contribute as well with significant fractions to the carbon load in PM.

In recent years scientific research has focused on carbonaceous particles due to their impact on climate and human health (Ramana et al., 2010; Shindell et al., 2012). Carbonaceous aerosols contribute substantially to the absorption and scattering of radiation in the troposphere and cause direct radiative forcing, e.g. BC absorbs sunlight thus heating the atmosphere, whereas most organic aerosol components have the opposite effect (Kanakidou et al., 2005; Ramanathan and Carmichael, 2008). A number of studies strongly suggest a link between carbonaceous aerosols and many health effects of airborne particles. EC concentrations have been used as a surrogate for exposure to diesel exhaust (Birch and Cary, 1996) with these emissions enhancing immunological responses to allergens and eliciting inflammatory reactions with impact on the respiratory and cardiovascular systems at relatively low concentrations and short exposure durations (Brunekreef et al., 1997). Organic aerosols may also pose a significant risk to human health (Mauderly and Chow, 2008; Verma et al., 2009).

Real time BC measurements are performed by using optical methods which measure the attenuation of light through a filter collecting airborne particles. The most commonly used methods include the Aethalometer (Magee Scientific, Berkeley, USA, Hansen et al., 1984), the Particle Soot Absorption Photometer, PSAP (Bond et al., 1999) and the Multi Angle Absorption Photometer, MAAP (Petzold and Schönlinner, 2004). Despite intensive efforts over the last decades, no widely accepted standard measurement method exists for the determination of BC or light absorbing carbon, although several intercomparisons have been carried out (Chow et al., 2009; Müller et al., 2011). Following suggestions by the GAW Scientific Advisory Group (GAW/WMO, 2011), the term “Equivalent Black Carbon” (EBC) should be used instead of Black Carbon for measurements derived from optical methods. Much care must be taken in deriving EBC from light absorption measurements, and the conversion factors used should be always supplied with the data.

Thermal-optical analysis has been widely used for the determination of OC and EC in atmospheric aerosol samples (Phuah et al., 2009). According to this method, OC desorbs in an inert atmosphere (He) while EC combusts in an oxidizing atmosphere (mixture of He and O_2) at high temperature. However, some OC is pyrolytically converted to EC (char) when heated up in He. This process darkens the filter, and this darkening is used to correct for charring by continuously monitoring the transmittance (or reflectance) of the filter during the analysis (Birch and Cary, 1996). The most commonly employed thermal protocols are IMPROVE (Chow et al., 1993), NIOSH (Birch and Cary, 1996) and EUSAAR2 (Cavalli et al., 2010). Thermal-optical analysis can also be used for the determination of CC which is usually not considered in atmospheric

Title Page
Abstract | Introduction
Conclusions | References
Tables | Figures
◀| |▶
◀ ▶
Back | Close
Full Screen / Esc
Printer-friendly Version
Interactive Discussion

studies. Recently Karanasiou et al. (2011) reported on the possibility of identifying and quantifying atmospheric CC using a thermal-optical transmission analyzer.

Collecting particles on filters for offline or online thermo-optical analysis potentially leads to sampling artifacts. Positive OC artifacts arise from organic vapor adsorption onto quartz-fiber filter material and/or previously collected particles (matrix), leading to an overestimation of particulate OC (Turpin et al., 2000; Mader et al., 2001). Negative artifacts can be caused by volatilization of organic particle-phase semivolatile compounds from the filter into the gas phase, leading to an underestimation of OC (Subramanian et al., 2004; Arhami et al., 2006). As an example, in the Barcelona urban area, positive artifacts for OC account for 0.5–0.7 $\mu g\,m^{-3}$, representing 11–16 % of the bulk OC mass and 3 % of the $PM_{2.5}$ mass, and are slightly higher in summer when compared to winter (Viana et al., 2006).

According to previous studies (Querol et al., 2008) nmC accounts for 10–22 % of PM_{10} in the rural background, 10–27 % in the urban background and 20–32 % at traffic/kerbside sites. These percentages increase to 25–28 % (rural), 21–37 % (urban) and 32–42 % (kerbside) in $PM_{2.5}$.

Given the high variability of sources, carbonaceous aerosols comprise a great variety of compounds with different climatic and health effects. State of the art techniques permit us, at least in theory, to determine in real time ambient air concentrations of organic species. However, economic restrictions and technical requirements hinder the use of these new technologies for AQ networks. Determination of OC and EC concentrations can be subject to a high uncertainty due to problems with sampling artifacts and differences between methods or techniques (Putaud et al., 2011). Real time monitoring of EBC also depends on the measurement technique, but has been proved to be a good proxy for monitoring the impact of traffic emissions in AQ in urban areas.

This work focuses on the characteristics, trends and sources of carbonaceous aerosols in urban, traffic, industrial, rural and remote sites in Spain (Western Mediterranean). The objectives of this study are to interpret the temporal and spatial variability of ambient air concentrations of particulate non-mineral carbon, OC, EC and EBC across Spain. To this end, data obtained with similar methods at 78 monitoring sites across the country during the period 1999–2011 were compiled and interpreted. We focus on: (a) mean concentration ranges for nmC, OC, EC and EBC; (b) inter-annual and seasonal trends; (c) OC/EC ratios; (d) EBC/EC ratios; (e) possible origins for OC and EC. Finally, we discuss the feasibility and usefulness of measuring and regulating the concentrations of these PM components.

2 Methodology

2.1 Sampling

During the period 1999–2011 nmC concentrations were determined at 78 monitoring stations across mainland Spain, the Balearic and Canary Archipelagos and the Spanish Northern African territories (Fig. 1 and Table 1). OC and EC concentrations were available for 33 sites. The analyses were carried out in PM_{10} and $PM_{2.5}$ 24h samples. Table 1 shows the nmC, OC, EC and EBC mean concentrations for specific periods (in most cases covering > 1 yr) in the following sites (see also Supplement S1 for more details):

- 2 mountain remote sites: Montsec and Izaña.
- 10 rural/regional background sites: Montseny, Monagrega, Bemantes, El Perdón, Endrinal Cortijo, San Jorge, Matalascañas, Valverde del Camino, Campillos and Can Llompart.
- 10 industrial-suburban sites: Ponferrada, Plaza Castillo-Almería, Poblado-Córdoba, Torrelavega, Monzón, Alacant, Onda, Arenosillo, Punta Umbria and Santa Cruz.

- 20 industrial urban sites: Tarragona, Puertollano, Huelva, La Línea, Puente Mayorga, Los Barrios, Bailén, Alcalá de Guadaira, L'Alcora, Vila-real, Borriana, Almassora, Agost, Llodio, Bajo Cadagua, Zabalgarbi, Alsasua, Avilés, Torredonjimeno and Montcada.
- 7 suburban sites: Palma de Mallorca, Chapinería, Burgos, Badajoz, Santa Ana-Cartagena, El Vacar-Córdoba and Nerva-Huelva. These are stations located in the outskirts of cities or villages.
- 19 urban background sites: Granada, Moguer, Cádiz, Córdoba, Sevilla, Jaén, Melilla, Las Palmas de Gran Canaria, Albacete, Alcobendas, Madrid, Barcelona, Sabadell, Girona, Zaragoza, Bilbao (2 sites), Pamplona and Santander.
- 10 road traffic sites: Sabadell, Girona, Barcelona, Madrid, Granada, Almería, Málaga-Carranque, Cartagena, Barreda-Torrelavega and Bilbao.

Total carbon, OC and EC measurements were carried out on PM_x samples collected on filters by high or low volume samplers. To this end microfiber quartz filters from different brands were used along 1999–2011, including Schleicher & Schuell, Munktell and Pallflex, after a 200 °C treatment. The only exception is for the monitoring site in Madrid where online techniques were applied for OC and EC measurements. The online EBC measurements were carried out at 6 sites (Barcelona, Huelva, Santa Cruz, Granada, Montseny and Montsec).

2.2 nmC determinations

The nmC contents were obtained by subtracting the mineral or carbonate carbon (CC) from the total carbon (totalC) determined by means of classical elemental analysis. The total C was determined in a circular fraction (of 2.54 cm diameter) of the corresponding PM_x filter with elemental analyzers using a few milligrams of V_2O_5 as an oxidant agent. The CC was stoichiometrically obtained from the Ca and Mg concentrations determined in the same filters by assuming that these two elements are present as calcite and/or dolomite ($CaCO_3$ and $CaMg(CO_3)_2$). The recovery, LOD and uncertainties of the method are the ones typical for elemental analyzers. When only thermo-optical method was used for the analysis of the carbonaceous aerosols nmC was obtained as the sum OC + EC, without any subtraction of CC. In any case, mean CC concentrations were generally low (e.g. 9 and 2 % of total C in PM_{10} and $PM_{2.5}$, respectively, in Barcelona).

2.3 EC and OC determinations

Concentrations of OC and EC were determined on the PM_x filters by the Thermal–Optical transmission method (TOT).

Filters from Monagrega and Barcelona-traffic in 1999–2000, as well as those from Huelva, Arenosillo, La Línea and Bailén in the period June 2005-June 2006, were analysed in the Laboratories of the Aveiro University using the TOT protocol described by Pio et al. (1994). The method consists of a quartz tube with two heating zones, a laser and a detector for the laser beam, and a CO_2 analyzer. A circular section of the sampled quartz filter 9 mm in diameter is placed vertically inside a quartz tube oven and heated to 600 °C in a nitrogen atmosphere to vaporize organic carbon. A second heating zone is filled with cupric oxide and maintained at 650 °C during the entire analysis process to guarantee the total oxidation of the volatilized carbon to CO_2, which is analyzed by a non dispersive infrared detector (NDIR). Controlled heating is used in steps to separate OC into four fractions of increasing volatility of lower and higher molecular weight organics, as follows: step1 ($T \leq 150\,^{\circ}$C, OC1); step2 ($T \leq 150$–$350\,^{\circ}$C, OC2); and step3 ($T \leq 350$–$600\,^{\circ}$C, OC3). Elemental carbon is determined by sequential heating at 850 °C in a nitrogen and air atmosphere (step4). A laser beam is used to differentiate between OC and EC, based on filter light transmittance, similar to other thermal–optical methods. Intercomparison data showed that the Aveiro University methodology correlates very well with the EUSAAR2 protocol (Supplement, Fig. S2).

The remaining filter samples were analyzed using TOT Sunset Laboratory instruments at the IDAEA-CSIC laboratory in Barcelona and the Carlos III Health Institute in Madrid, from 2007 to present. A NIOSH-like thermal protocol adequate for the offline Sunset analyzer (known as Quartz.par) was used in an initial phase and the EUSAAR2 protocol was used from July 2008 onwards. Only OCEC data from Barcelona 2004–2006 were obtained using a Sunset OCEC Analyzer at Ghent University using also the Quartz protocol (Viana et al., 2006). The Quartz protocol is a NIOSH-like protocol as described in the European guide CEN/TR 16243: 2011, and it is widely used by researchers (e.g.: Schmid et al., 2001; Schauer et al., 2003; Viana et al., 2007; Koulouri et al., 2008; Bae et al., 2009). It is the protocol of a subsequent version provided by the instrument's manufacturer (Birch and Cary, 1996), and it is commonly referred in the literature as modified "NIOSH" protocol, being directly comparable to the NIOSH 5040 or NIOSH/EPA thermal protocols (Cavalli et al., 2010).

For the TOT method with the Sunset analysers (Birch and Cary, 1996), a punch (typically 1.5 cm^2) of a quartz fibre filter sample is placed in the quartz oven of the instrument. In the initial phase of the analysis, which takes place in a pure He gas stream, the filter punch is heated in different series of steps (according to the different temperature protocols), the desorbed carbonaceous vapours are catalytically oxidised into CO_2 (by a MnO_2 catalyst), the CO_2 formed is reduced to CH_4 (in a Ni-firebrick methanator oven) and the latter is subsequently measured with a flame ionisation detector (FID). Laser light of 670 nm is passed through the filter punch and the light transmission is continuously measured, in order to correct for pyrolysed OC. In the second phase, which takes place with a 98 %He/2 %O_2 mixture as carrier gas, the filter punch is further heated, and the CO_2 evolved is measured by FID in the form of CH_4 (as in the first phase). When the light transmission through the filter punch equals that seen at the beginning of the first phase, the OC/EC split is set to correct for pyrolytic carbon (PC): the CO_2 measured in the first phase and during the second phase prior to the split is considered OC (including the PC), whereas the CO_2 measured after the split is considered the "real" EC. After the end of the second phase, while still in a He/O_2

mixture, a known amount of CH_4 gas is injected through a loop for internal calibration. The Quartz and the EUSAAR2 thermal protocols are described in Table S1.

Finally, EC and OC at the urban background site in Madrid were determined on a semi-continuous basis by a thermal analyzer (Ambient Carbonaceous Particle Monitor-ACPM, Rupprecht and Patashnick model 5400, Thermo Scientific Inc.). This online analyzer collects $PM_{2.5}$ onto an impactor plate prior to the sequential heating/oxidation. CO_2 concentrations from this oxidation are analyzed online. Two sequential heating/combustion steps, at 340 °C and 750 °C are used to separate and determine OC and EC fractions, respectively. The use of ambient air as oxidant for both carbonaceous fractions minimizes the pyrolysis of OC, thus avoiding the need to apply charring correction factors. The instrument has been compared with results of collocated filter sampling and subsequent offline TOT analysis at Aveiro University and data were corrected according to the results of this comparison (Plaza et al., 2011).

The assessment of the comparability between the different thermal protocols used is not the objective of the present work, as numerous studies have already addressed it (Cavalli et al., 2010; Subramanian et al., 2006; Chow et al., 2001, 2004; Conny et al., 2003; Schauer et al., 2003; Schmid et al., 2001). In Europe mainly the EUSAAR2 and NIOSH protocols are used. The authors are aware that this is a limitation of the study, which is accounted for in the discussion (see sections below). The scope of the paper is, conversely, to report and discuss the characteristics, trends and sources of carbonaceous aerosols from long term measurements across Spain.

2.4 Online EBC measurements

Hourly EBC concentrations (at $\lambda = 637\,\mathrm{nm}$) were measured for at least one year at the 6 sites shown in Table 1 by means of a Multi Angle Absorption Photometer (MAAP, model 5012 Thermo Scientific). The EBC concentration provided by MAAP is calculated by the instrument's software as EBC [$\mathrm{g\,m^{-3}}$] = $\sigma_{ap}(\lambda)$ [$\mathrm{m^{-1}}$] / $\sigma(\lambda)$ [$\mathrm{m^2\,g^{-1}}$] (Petzold and Schönlinner, 2004), where $\sigma_{ap}(\lambda)$ is the measured absorption coefficient and $\sigma(\lambda)$ is the mass absorption cross section (MAC). The default MAC used by the instrument is

6.6 m^2 g^{-1}, which is the MAC at 637 nm (Müller et al., 2011) recommended by the manufacturer.

The values of MAC may vary as a function of the aerosol composition and age, and therefore they can differ depending on the area under study and meteorological scenarios. Mass absorption cross sections (MAC) between 7 m^2 g^{-1} and 15 m^2 g^{-1} have been usually reported in the literature (e.g. Bond and Bergstrom, 2006; Fernández-Camacho et al., 2010; He et al., 2009; Barnard et al., 2008; Arnott et al., 2003, 2005; Reche et al., 2011). MACs obtained at the present study are shown in the Fig. S1, as the slope of the regression equation between the absorption coefficient and the concentrations of EC determined from filters by the thermo optical method. Results evidenced MACs around 10 m^2 g^{-1} in urban and rural sites, showing a higher variation in remote locations.

Nevertheless, in order to facilitate comparison with measurements recorded at other areas, the EBC concentrations shown in the present paper are those directly provided by the MAAP instruments (i.e. after applying a default value of 6.6 m^2 g^{-1}). Thus, according to the above MACs values, EBC data here presented may be overestimated by 30–35 %.

2.5 Limitations of the methods used

The results and discussions presented are subject to a number of limitations, some of which are intrinsic to the methodologies used and are well-documented in the literature. Below we highlight the most relevant limiting factors.

- Not all measurements (neither sampling nor analytical) were conducted simultaneously at all the study locations. This implies that the results may not always be directly comparable.

- Not all thermo-optical analyses were carried out using the same temperature protocol: whereas a fraction of the analyses were carried out using Quartz (the NIOSH-like) protocol, the most recent ones used EUSAAR2 protocol. A recent intercomparison showed that the EUSAAR2 protocol systematically leads to lower EC values compared to the NIOSH derived protocols (Maenhaut et al., 2012, conference presentation). In some cases, such as Barcelona and Montseny, two protocols have been used along the time series and this may have influenced artificially time trends of OC and EC levels, but probably not much those of OC + EC or nmC levels. That is why our time trend analysis focuses mostly on nmC (or OC + EC).

- The determination of nmC based on Ca and Mg concentrations implies an error that is difficult to estimate. Ca and Mg may be present in mineral dust in forms other than calcite and dolomite, e.g. a small fraction of Ca in soils may be present in oxide forms (not as carbonate species) and Mg can be of sea salt origin. Furthermore, even when dust soil particles are emitted as carbonates, inter-reaction in the atmosphere with SO_2, H_2SO_4 and HNO_3 has a tendency to transform those into sulfate and nitrate species. Therefore, the use of Ca and Mg as tracers may result in an underestimation of nmC levels, but in any case calculated CC concentrations are low when compared with nmC (e.g. 2–9 % of total C in Barcelona).

- The determination of OC and EC comprises an intrinsic degree of uncertainty arising from the selection (whether automatic or manual) of the split point (Cavalli et al., 2010). The split between OC and EC is temperature protocol dependent, and in addition it is highly sensitive to the morphology of the C peaks during the analysis. A slight shift of the split point may result, on occasions, in large changes in the OC/EC ratio. As reported in Subramanian et al. (2006), 15 $\mu g\,cm^{-2}$ as the EC loading on a filter is a limit for assessing a good performance of the Sunset (TOT) instrument. With loadings > 15 $\mu g\,cm^{-2}$, the laser signal passing through the filter is so low that no signal modulation for higher EC loadings can be detected during the He phase, and no correction for pyrolysis can therefore be performed. As a result, exceeding the 15 $\mu g\,cm^{-2}$ would have a direct impact on the OC/EC ratio. During our study, this limit was not exceeded. Furthermore, the presence of high concentrations of iron oxides (or other metal oxides) may act as a catalyst or oxygen donors during the He-phase in the TOT analysis. Wang et al. (2010) evidenced that metals reduce the oxidation temperature of EC and enhance the charring of OC. The split point used to determine classification of EC vs. OC may thus be more dependent on changes in EC oxidation temperature than on charring. This artifact are protocol-dependent, i.e. their extent depends on the use of the NIOSH, IMPROVE or EUSAAR2 protocols (Chow et al., 2004). In the present study, only samples from the background site of Izaña may have been affected by this artifact.

- The presence of carbonates in the sample could lead to an overestimation of the OC when EUSAAR2 or NIOSH-like thermal protocols are used. In this study CC was not removed prior to the analysis by, e.g.: acidification with HCl or phosphoric acid. As a result CC might interfere with the determination of OC or EC, depending on the carbonate characteristics, and on the thermal protocol used (Karanasiou et al., 2011).

- Positive and negative sampling artifacts were not taken into account in the present study, since neither denuders nor impregnated filter packs were used during sampling. In most cases, high-volume samplers were used in which the high face velocity (74 cm s^{-1}, as opposed to 22 cm s^{-1} for low-volume samplers, Viana et al., 2006) minimized the impact of positive OC artifacts (Turpin et al., 2000). In any case, tests carried out with low-volume samplers in Ghent, Amsterdam and Barcelona (Viana et al., 2007) evidenced that positive sampling artifacts ranged from 5–7 % of the OC concentration in Ghent to 11–16 % in Barcelona. They also found that artifacts were most likely higher in Southern than in Western Europe, as a consequence of higher ambient temperatures and the enhanced emission of VOCs. This may also be applied to Spain where an intense climate gradient occurs. Longer sampling periods and higher filter loads have a tendency to reduce OC positive artifacts as a result of saturation of adsorbing active quartz filter surfaces. On the other hand long sampling periods are prone to interferences from atmospheric changing equilibrium conditions. Recently, positive artifacts were estimated to account for 29 % of total C at the regional background station of Montseny in the framework of the EUSAAR project (www.eusaar.net; unpublished data), but this was obtained by using low volume samplers. A low proportion is expected in the urban areas due to higher absolute OC particulate levels and using high volume samplers (Maenhaut et al., 2001). In any case positive and negative sampling artifacts may have a different impact in urban or rural environments, and may be higher in urban environments (Chow et al., 2010).

- A major limitation of the discussion is that we may in some cases compare EC, OC and EBC nmC from PM_{10} and $PM_{2.5.}$ This may not be completely accurate for OC and probably less significant for EC and EBC. Most of the data refers to $PM_{2.5}$ and only include PM_{10} when the first is not available. Although we are aware that OC in $PM_{2.5}$ may be lower than in PM_{10} we still included PM_{10} data with the aim of a higher spatial coverage. As an indicator of the difference this may suppose that OC mean annual levels decrease from PM_{10} to $PM_{2.5}$ by 10 and 12 %, for Montseny and Barcelona, respectively. For EC the decrease is around 9 and 17 %, respectively.

2.6 Temporal trends

Temporal trends were analyzed at the monitoring sites where at least 4 yr of data were available. The Theil-Sen method (Theil, 1950; Sen, 1968), available in the Openair software (Carslaw, 2012; Carslaw and Ropkins, 2012), was applied to the monthly averages to calculate the regression parameters of the trends including slope, uncertainty in the slope and the *p* value. The applied method yields accurate confidence intervals even with non-normal data and it is less sensitive to outliers and missing values (Hollander and Wolfe, 1999). Data were deseasonalized and all the regression parameters were estimated through bootstrap resampling. The slopes indicate how concentrations have changed through time and are expressed in units ($\mu g\,m^{-3}$ in our case) per year. The p values show whether the calculated trends are statistically significant. A statistically significant trend was assumed at the 90th percentile significance level ($p < 0.1$), meaning that there was a 90 % chance that the slope was not due to random chance. p values > 0.1 and ≤ 0.01 indicate insignificant and highly significant trends, respectively.

3 Results

3.1 nmC concentrations

Figures 2 and 3 show the mean annual concentrations of nmC measured at the 78 sites ordered from the lowest to the highest concentration. Data did not evidence any spatial trends of carbonaceous aerosols across Spain. Conversely, an increase by a factor of 5 is evidenced from remote, rural to traffic and industrial sites. The following nmC concentration ranges may be deduced from these figures:

- Remote sites: 1.1–1.3 $\mu g\,m^{-3}$.
- Rural sites: 1.8–2.6 $\mu g\,m^{-3}$ for most sites, with one site (Bemantes) reaching higher levels (3.5 $\mu g\,m^{-3}$) probably due to higher emissions from regional domestic and agricultural biomass combustion and forest fires.
- Industrial sites: 3.3–7.0 $\mu g\,m^{-3}$ for most sites, depending on the type of industry, but with mean concentrations exceeding 5 $\mu g\,m^{3}$ in petrochemical and coke estates or industrial-urban sites. In Bailén, concentrations reached anomalously high values (10.6 $\mu g\,m^{-3}$) due to the large emissions from numerous old manufacturing installations of bricks and pottery. Conversely, one suburban industrial site (Plaza Castillo-Almeria) oriented to monitor the impact of power generation, and a harbour-influenced site (Santa Cruz) recorded relatively low concentrations (1.8 $\mu g\,m^{-3}$).

- Urban and suburban background sites: 3.0–6.5 µg m^{-3} for most sites.

- Traffic sites: 4.4–5.9 µg m^{-3} at five small- or medium-sized cities (Granada, Almería, Carrenque, Torrelavega Barreda and Bilbao), and 8.3–10.3 µg m^{-3} in the larger and/or more industrialized cities (Madrid, Barcelona, Sabadell, Cartagena and Girona).

3.2 EC and OC concentrations

Annual average concentrations of EC (Figs. 3 and 4) markedly increased by a factor of up to 50 from remote to traffic and some industrial sites. According to the EC concentrations measured, the following ranges were evidenced:

- Remote sites: 0.07–0.13 µg m^{-3}.

- Rural sites: 0.2–0.3 µg m^{-3}.

- Industrial-rural sites: 0.5–0.9 µg m^{-3}.

- Industrial urban-sites: 0.8–1.0 µg m^{-3} in most sites, 1.7–2.3 µg m^{-3} in coke and metallurgical estates, and 3.1 µg m^{-3} in the above mentioned brick production estate with a large number of very old installations (Bailén).

- Urban background sites: 0.6–0.9 µg m^{-3} in small and midsized cities and 1.3–1.7 µg m^{-3} in the larger cities. Medium-sized cities Granada and Melilla also fall in the 1.3–1.7 µg m^{-3} range due to the location of the station (Granada) and to a large influence from shipping emissions and also transboundary EC pollution from the nearby Moroccan border (Melilla).

- Traffic sites: 1.4 µg m^{-3} in a small city (Barreda-Torrelavega) and 3.2–4.1 µg m^{-3} in the larger cities (Madrid, Sabadell).

For OC concentrations (Figs. 3 and 4) the range of variation is much narrower when compared with EC. The increase from remote to traffic sites reached only a factor of 5, ten times lower than that obtained for EC. According to the OC concentrations measured, the following ranges were evidenced:

- Remote sites: 1.1–1.6 $\mu g\,m^{-3}$.
- Rural sites: 2.0–2.3 $\mu g\,m^{-3}$.
- Industrial sites, including industrial-rural sites: 2.3–4.7 $\mu g\,m^{-3}$ in most cases, and 5.4 $\mu g\,m^{-3}$ in the brick production estate of Bailén.
- Urban background sites: 1.8–4.5 $\mu g\,m^{-3}$.
- Traffic sites: 3.6–5.4 $\mu g\,m^{-3}$.

Sampling artifacts for OC were not avoided with the methodology used; as previously stated (Viana et al., 2007), a rough estimation of around 10–15 % of the total OC (positive artifact) for low volume sampling can be assumed (this being much higher than for high volume samplers as described by Turpin et al., 2000). Thus, for a hypothetical extreme scenario in which a positive artifact of 15 % was assumed at traffic sites, and a negative artifact of 0 % was assumed at remote sites (Chow et al., 2010), the above mentioned traffic/remote factor for OC would decrease to 4. As a result, the difference regarding the traffic/remote factor for EC (up to 50) would be even larger if sampling artifacts were taken into account.

As expected OC/EC annual ratios (Fig. 5) markedly decreased by a factor of 10 from the remote to traffic and some industrial sites. According to the ratios measured, the following ranges were evidenced:

- Remote sites: 12–15.
- Rural sites: 8–11.
- Industrial-rural sites 5–8.

- Most industrial sites: 2.3–4.1. Lower ratios (1.6–1.9) were found at coke and metallurgy hotspots, and 0.8 in the harbor site influenced by road traffic and an old petrochemical plant (Santa Cruz).
- Urban background sites: 4.0–5.6 in the small cities (Albacete, Zaragoza and Santander) and 2.0–3.2 in the larger and/or more industrialized/trafficked sites such as Madrid, Barcelona, Sabadell, Granada and Melilla. In Melilla the low OC/EC ratio may be due to the high influence of shipping emissions, increasing the EC concentrations, in this site close to the Gibraltar Strait (and to transboundary pollution across the Moroccan border).
- Traffic sites: 1.6–1.7 in large cities, around 2.5 in small cities.

3.3 Inter-annual trends

Decreasing trends for carbonaceous compounds were observed at almost all the stations through time, with significance levels p ranging from 0.001 to 0.1 in many cases, and with more significant and robust results obtained for stations with more than 5 yr of measurements. This is now discussed in more detail for each type of site. Figure 6 shows some examples of the temporal trends for selected stations as representative of regional (Montseny), urban (Barcelona), industrial (Bailén), urban-industrial (Huelva) and suburban-industrial (Santa Cruz de Tenerife) environments.

Remote background (Montsec): the concentrations of nmC did not exhibit definite trends (2006–2011), likely due to the position of this monitoring station (1570 m a.s.l.), often above the planetary boundary layer, making anthropogenic-driven trends more diluted when compared with other stations in Spain.

Regional background (Montseny): significant decreases were observed for nmC ($p = 0.01$) and OC ($p = 0.001$) concentrations in $PM_{2.5}$ during the period 2002–2010. Both nmC and OC concentrations decreased at a rate of around $-0.2\,\mu g\,m^{-3}\,yr^{-1}$ (Fig. 6), which is equivalent to a decrease of $1.4\,\mu g\,m^{-3}$ and $1.3\,\mu g\,m^{-3}$ for nmC and OC, respectively, between 2002 and 2010. No significant trend was observed for EC concentrations (data not shown). However, the annual mean EC concentrations at Montseny were very low – ranging between 0.2 $\mu g\,m^{-3}$ and 0.3 $\mu g\,m^{3}$ in the 2002–2010 period – and highly influenced by the split point that depends on the measurement protocol used.

Urban background (Barcelona): over the period 2003–2010 a significant decreasing trend was observed for nmC in $PM_{2.5}$ at a rate of $-0.7\,\mu g\,m^{-3}\,yr^{-1}$ (around 50 % decrease at $p = 0.001$) (Fig. 6). In absolute terms, this decrease was equivalent to $3.6\,\mu g\,m^{-3}$ from 2003 to 2010. Significant decreases of nmC concentrations (31–35 %) were also detected at other urban background sites (Granada, Córdoba, Cádiz, Jaén, Sevilla, Málaga). Similarly, statistically significant ($p < 0.01$) trends were detected for OC and EC between 2007 and 2010. The OC/EC ratio in Barcelona over the 2007–2010 increased (at $p = 0.001$) at the rate of $0.3\,\mu g\,m^{-3}\,yr^{-1}$ indicating a higher relative decreasing rate of EC compared with OC in Barcelona.

Traffic sites (Madrid): nmC concentrations in $PM_{2.5}$ were only available for the years 2000, 2007 and 2011, thus data were not sufficient for the application of the Theil–Sen method. A simple linear regression applied to the data showed a decreasing trend for nmC concentrations at a rate of $-0.7\,\mu g\,m^{-3}\,yr^{-1}$, which is similar to the decreasing rate observed for nmC in Barcelona, with a regression coefficient R^2 of 0.99.

Urban/industrial sites: with the exception of Huelva, at most sites clear decreasing trends were evidenced for nmC for both PM_{10} and $PM_{2.5.}$ For the period 2007–2010, decreasing trends were obtained ranging from $-0.2\,\mu g\,m^{-3}\,yr^{-1}$ to $-0.6\,\mu g\,m^{-3}\,yr^{-1}$, (18–27 % decreases, 1.8–2.5 $\mu g\,m^{3}$ in total). For these stations the observed decreasing trends were less significant ($0.01 < p \leq 0.1$) compared to urban sites. The strongest decrease in nmC concentrations was registered in Bailén over the period 2004–2010 at a rate of $-0.9\,\mu g\,m^{-3}\,yr^{-1}$ (around 50 % or 6.90 $\mu g\,m^{-3}$) (Fig. 6), due to the reduction in brick manufacture activities caused by the financial crisis.

The only site where nmC concentrations did not decrease but instead remained almost constant between 2000 and 2010 was Huelva (urban-industrial, Fig. 6). Conversely, nmC levels showed increasing trends only at two sites (Matalascañas regional background and Plaza Castillo-Almería power generation-regional background), with increases ranging between 0.1 and 0.4 µg m^{-3} yr^{-1}.

4 Discussion

4.1 Ambient concentrations of carbonaceous aerosols

The spatial variability of nmC across different atmospheric environments in this study shows that anthropogenic carbonaceous aerosols in Spain within the period 1999–2010 mainly originated from road traffic and in a minor proportion from biomass burning (anthropogenic and wild fires, and agricultural biomass burning), and industrial and shipping emissions. Urban air pollution is markedly dominated by emissions from vehicular traffic, with the major Spanish cities (especially Barcelona) suffering from the highest vehicle density, with a high proportion of diesel cars, in Europe. Naturally emitted carbonaceous aerosols (both primary and secondary) may also be considered significant in the regional background especially in spring and summer (Seco et al., 2011; Minguillón et al., 2011), especially in the central and northern regions of the Iberian Peninsula.

Reviewing the carbonaceous aerosol concentrations in $PM_{2.5}$ across Spain, mean annual concentrations of nmC range from around 1 µg m^{-3} at the most remote and pristine sites, to around 10 µg m^{-3} in the most polluted cities. Petrochemical and coke estates provide notable industrial point sources of nmC, and biomass burning (domestic, agricultural and forest fires) is probably causing an increase of around 1 µg m^{-3} in the annual nmC mean at regional background sites in northern Spain with respect to the rest of the Spanish territory.

The OC and EC data similarly show marked differences from remote to traffic sites (1.1–1.6 µg m^{-3} of OC; OC/EC = 12–15 compared with 3.8–5.4 µg m^{-3} of OC; OC/EC = 1.0–1.7, respectively). This reflects the impact of emissions from traffic and specific industrial processes. However, the OC concentration range is much narrower than for

EC, as the increase in OC concentrations from remote to traffic sites reached only a factor of 5 (much lower than 50 for EC).

Plotting OC/EC average ratio against EC concentrations (Fig. 7) shows similar results to those obtained by Pio et al. (2007, 2011), but in this study the higher influence of biomass burning emissions provoked a higher OC/EC ratio. As shown in Fig. 7, correlation between yearly averaged OC/EC and EC concentrations adjusts very well to a potential equation ($y = 3.37x^{-0.67}$ $R^2 = 0.94$). A similar equation is obtained when including average concentrations obtained at other European sites ($y = 3.61x^{-0.5}$ $R^2 = 0.78$) shown by Pio et al. (2007 and 2011), Ytri et al. (2007), Spindler et al. (2010), Grivas et al. (2012) and references therein. Stations in the right end of the fitting curve correspond with traffic sites. The left site of the curve is occupied by values from remote sites. Values of the above the curve usually have a high influence from biomass burning, whereas most values on the curve or below the curve correspond to traffic influenced urban sites and industrial sites. These data may be very useful for the modeling community.

Recent data on ^{14}C at Barcelona (Minguillón et al., 2011) showed a high proportion of non fossil OC (52–60 %) in the urban background. This probably indicates that a large proportion of urban Secondary Organic Carbon (SOC) can be formed inside the city from regional VOCs (with a high proportion of biogenic VOCs) due to the oxidative environment created by urban pollution. Other contributions to modern OC, such as the contribution of cooking aerosols identified in Barcelona by Mohr et al. (2012), cannot be discarded. However, their mass contribution is still unclear.

The slope of the regression equation between OC and EC is very high (8) for the remote and rural sites and progressively lower as EC increases towards the industrial (1.2) and urban and traffic sites (0.8). Pio et al. (2011) found minimum OC/EC ratios (attributed to primary traffic contributions) at urban background sites in Europe to be around 0.7 in $PM_{2.5}$ and 1.0 in PM_{10}, which is similar to our urban OC/EC slope. It is also close to the OC/EC ratio determined at the Atlantic island site of Santa Cruz de Tenerife (0.8), which very probably reflects a primary traffic ratio. According to our results the OC/EC ratios of the regression equations are 7–10 times higher in the remote and regional background sites than in the urban and industrial areas.

Thus, the high correlation observed between OC and EC across Europe, especially for rural background sites independently of vegetation type, climate and photochemistry, is surprising. Although correlation is also good for urban, traffic and industrial sites, the correlation between OC and EC concentrations is not as marked as for the rural sites, probably due to the different impact of biomass burning and traffic/industrial sources. The OC/EC ratio usually depends on the type of fuel, being higher for biomass and lower for fossil fuel (Novakov et al., 2000; Szidat et al., 2007).

4.2 Inter-annual trends

One especially interesting finding was the decreasing annual trends observed at almost all the stations and station types. The decreasing trend of OC + EC (or nmC) of -0.4 to $-0.7\,\mu\mathrm{g\,m^{-3}\,yr^{-1}}$ measured at the largest cities in Spain may be consequence of the implementation of environmental action plans or legislation, such as EURO4 and EURO5 standards to reduce diesel PM emissions, or the European Directive 1996/61/EC (IPPC Directive: Integrated Pollution Prevention and Control) on the reduction of industrial emissions. Slightly higher decreasing trends may be due to local effects (as found in Madrid, probably related to the change in the traffic regime in the proximity of this site due to the construction of a tunnel). In the last years, the financial crisis may have also influenced these trends, although these were already present before 2008 when the crisis started. Increasing or constant nmC concentrations were only found in very specific industrial influenced areas. This overall improvement in air quality is especially well demonstrated at stations with more than 5 yr of measurements, and emphasizes the value of obtaining continuous, long-term monitoring databases.

4.3 Seasonal trends

A distinct seasonal variability was found regarding OC and EC concentrations at traffic, urban, regional and remote background sites. As examples we describe seasonal patterns at the following selected sites: (a) one traffic site (Madrid); (b) one urban background site (Barcelona), (c) one regional (Montseny) and (d) one remote site (Montsec) (Fig. 8).

OC concentrations were higher during winter at the traffic and urban sites, decreasing during the warmer months. The higher OC concentrations measured during winter may be related to atmospheric conditions, as important anticyclonic episodes are usually recorded over the Iberian Peninsula during winter, producing the accumulation of pollutants in the vicinity of their emission sources (mainly vehicular emissions at traffic and urban sites). In addition, the lower temperatures prevent semivolatile organic compounds from volatilizing.

Conversely, OC concentrations at the remote and rural sites increased during the warmer months. This is mainly related to the increase of biogenic emissions during summer (Seco et al., 2011) but also to the summer atmospheric conditions, favoring higher photochemistry (higher O_3, UV and T coincident with enhanced biogenic emissions of VOCs) and recirculation of air masses over the area (Pérez et al., 2008).

For EC the seasonal variability is similar to OC for the traffic and urban sites, with higher concentrations recorded during the winter. This similar pattern for OC and EC is consistent with the OC/EC ratios found for urban and traffic sites, similar to those of primary traffic emissions. Hence, it is possible to conclude that the variation of OC and EC concentrations is mainly driven by dispersion conditions. At the regional site (Montseny), EC concentrations are characterized by higher concentrations in winter and in September–October. Such higher concentrations during winter are attributed to the influence of winter regional pollution episodes (Pey et al., 2010), whereas the September–October higher concentrations are related with other causes (agricultural biomass burning or other regional sources). At the remote site (Montsec), the only clear increase in EC concentrations was recorded in September, probably associated with agricultural biomass burning. No clear maxima were observed in winter, given that the monitoring site lies most of the time above the mixing boundary layer.

4.4 Daily and weekly evolution

Clear differences can be observed in the hourly evolution of EBC in different types of environment (Fig. 9). At urban sites (Barcelona and Granada), EBC concentrations trace road traffic contributions accurately. Two distinct maxima are typically observed in working days at morning and evening rush hours (07:00 and 19:00 UTC). This daily pattern varies proportionally to those of primary gaseous emissions from road traffic such as CO and NO_x (data not shown). The EBC/CO and EBC/NO_x ratios, however, are not constant among different sites due to different emission and dispersion patterns (Reche et al., 2011). A significant drop of EBC concentrations on weekends due to the reduced emissions from human activity is shown at urban and rural sites. Interestingly, the lowering in EBC concentrations, although smoother and with one-day of delay, is also observed at the remote site.

At rural and remote sites, EBC peaks only once (in the afternoon) with this maximum corresponding to the arrival of pollution from the emission area, by means of mountain breezes. The distance to the emission sources seems to drive the variance of EBC concentrations. The relative variation of the hourly mean values is higher at remote and rural sites (Fig. 9), being progressively reduced as the distance to the source decreases (at the urban and urban-industrial sites). This is due to the cleansing effect of renewed air masses reaching rural sites that permit a large variability of EBC concentrations.

5 Conclusions

We interpreted variability of levels of carbonaceous aerosols based on large database from 78 monitoring stations across Spain. As expected data show marked differences in average concentrations from the cleanest, most remote sites to the highly polluted major cities. Thus, urban (and very specific industrial) pollution was found to markedly increase levels of carbonaceous aerosols in Spain, with much lower impact of biomass burning.

Correlations between yearly averaged OC/EC and EC concentrations fit very well with a potential equation ($y = 3.37x^{-0.67}$ $R^2 = 0.94$). A similar equation is obtained when including average concentrations obtained at other European sites ($y = 3.61x^{-0.50}$ $R^2 = 0.78$). Stations in the right end of the fitting curve correspond with traffic sites. The left site of the curve is occupied by values from remote sites. Values of the above the curve usually have a high influence from biomass burning, whereas most values on the curve or below the curve correspond to traffic influenced urban sites and industrial sites. These data may be very useful for the modeling community.

A clear seasonal variability in OC and EC concentrations was detected, with higher concentrations during winter at the traffic and urban sites and contrasting with OC at rural sites (increasing during the warmer months). Urban sites across Spain show classical patterns of hourly variations in EBC concentrations which accurately depict daily traffic flows, whereas a single midday pollution peak, commonly driven by outflows from nearby urban centres, characterises remote and rural sites.

One especially interesting finding was the decreasing annual trends observed at almost all the stations and station types. This may be consequence of the implementation of environmental action plans or legislation, such as EURO4 and EURO5 standards to reduce diesel PM emissions. In the last years, the financial crisis may have also influenced these trends, although these were already present before 2008 when the crisis started. Increasing or constant nmC concentrations were only found in very specific industrial influenced areas. In contrast with nmC, ambient air NO_2 trends in most EU large cities have not been seen to decrease as described here for nmC (Williams and Carslaw, 2011). This is highly relevant for air quality regulations since NO_2 has been considered a proxy of traffic-related PM. As shown in Fig. 10, in Barcelona the time trends of $NO_2/(OC+EC)$ have increased from around the value of 5 (2004) to the current value of 12 (2010).

5.1 Implications for air quality policy

WHO (2012) reported substantial health effects for BC or for the substances that condensate on the graphitized carbon indirectly measured by BC measurements. Furthermore, EBC variation reflects the impact of traffic emissions at urban sites, and can be considered as a good indicator of anthropogenic emissions at these sites. At regional and remote sites, variations of EBC may be attributed to other sources and processes, but average concentrations of EBC are considerably lower with minimum implications for air quality and health (even if with potential effects on climate). EBC showed a significant and constant correlation with EC at urban sites across Spain showing that, although both parameters are not the same, they may be considered as equivalent and, consequently, suitable for tracing the impact of anthropogenic emissions.

Currently no standardized methodology is available to determine EBC or EC, but WHO (2013) has already indicated the need to set up air quality guidelines for BC. As mentioned before, the determination of OC and EC by thermal-optical methods implies uncertainties arising from several factors, e.g.: the selection of the split point, selected thermal protocol and interference from carbonates (Cavalli et al., 2010; Karanasiou et al., 2011), among others. Measurement of EBC by absorption photometry needs to be corrected to ensure comparability (Muller et al., 2011). Correction algorithms are already available for some of these instruments.

It could be concluded that continuous monitoring of EBC by absorption photometers is an adequate strategy for Air Quality monitoring mainly at urban sites where this parameter can be considered as a good tracer of exposure to anthropogenic emission. In a technical report for the European Environmental Agency (EEA), it was concluded that EBC monitoring would be viable in current European air quality networks, where this type of instruments are already present (Viana et al., 2013). As recently reported by WHO (2012), there are sufficient evidences of the association between the cardiopulmonary morbidity and mortality with BC exposure. This review concluded that "a reduction in exposure to $PM_{2.5}$ containing BC and other combustion-related particulate material for which BC is an indirect indicator should lead to a reduction in the health effects associated with PM and simultaneously contribute to the mitigation of climate change".

However, OC, including secondary OC, also has a potential health impact. Verma et al. (2009) have shown for Los Angeles in summer that both primary and secondary organic particles possess high redox activity. Photochemical transformations of primary emissions through atmospheric aging enhance the toxicological effect of primary particles in terms of generating oxidative stress and leading to subsequent damage in cells. Our results showed that at rural sites there is a clear correlation between OC and EC concentrations. However, at urban sites the OC/EC ratio may vary considerably depending on the sources. Moreover, a rapid formation of secondary organic compounds was evidenced at the urban scale due to the oxidation of regional or local volatile organic compounds in the highly reactive urban environment. Consequently, the measurement of nmC (OC + EC) should be a good indicator for air quality monitoring, providing more valuable information than simply monitoring EBC, especially when a reduction of EBC levels is expected due to the effect of EURO5 standard emissions.

Supplementary material related to this article is available online at: http://www.atmos-chem-phys-discuss.net/13/6971/2013/acpd-13-6971-2013-supplement.pdf.

Acknowledgement. This study was supported by the Ministry of Agriculture, Food and the Environment of Spain and by the Ministry of Economy and Competitivity (MINECO) of Spain and FEDER funds under the project CARIATI (CGL2008-06294/CLI), VAMOS (CGL2010-19464/CLI), GRACCIE (CSD 2007-00067) and POLLINDUST (CGL2011-26259); and by AGAUR-Generalitat de Catalunya (2009 SGR 00008). The Montseny site forms part of the ACTRIS network (European Union Seventh Framework Program (FP7/2007–2013) project

No. 262254), formerly EUSAAR (EUSAAR R113-CT-2006-026140). Funding was also received for the Andalucía sites from projects 2007-RNM027329 and 2011-RNM7800: Department of Innovation Science and Enterprise, Andalusia Autonomous Government and the Project CGL2011-28025 from MINECO. M. C. Minguillón was funded by the JAE-Doc CSIC program, co-funded by the European Social Fund (ESF).

References

Aldabe, J., Elustondo, D., Santamaría, C., Lasheras, E., Pandolfi, M., Alastuey, A., Querol, X., and Santamaría, J. M.: Chemical characterisation and source apportionment of $PM_{2.5}$ and PM_{10} at rural, urban and traffic sites in Navarra (North of Spain), Atmos. Res., 102, 191–205, 2011.

Arhami, M., Kuhn, T., Fine, P. M., Delfino, R. J., and Sioutas, C.: Effects of sampling artifacts and operating parameters on the performance of a semicontinuous particulate elemental carbon/organic carbon monitor, Environ. Sci. Technol., 40, 945–954, 2006.

Arnott, W. P., Moosmüller, H., Sheridan, P. J., Ogren, J. A., Raspet, R., Slaton, W. V., Hand, J. L., Kreidenweis, S. M., and Collett Jr., J. L.: Photoacoustic and filter-based ambient aerosol light absorption measurements: instrument comparisons and the role of relative humidity, J. Geophys. Res., 108, 4034, doi:10.1029/2002JD002165, 2003.

Arnott, W. P., Hamasha, K., Moosmüller, H., Sheridan, P. J., and Ogren, J. A.: Towards aerosol light absorption measurements with a 7-wavelength aethalometer: evaluation with a photoacoustic instrument and 3 wavelength nephelometer, Aerosol Sci. Tech., 39, 17–29, 2005.

Bae, M.-S., Schauer, J. J., DeMinter, J. T., Turner, J. R., Smith, D., and Cary, R. A.: Validation of a semi-continuous instrument for elemental carbon and organic carbon using a thermal-optical method, Atmos. Environ., 38, 2885–2893, 2004.

Barnard, J. C., Volkamer, R., and Kassianov, E. I.: Estimation of the mass absorption cross 15 section of the organic carbon component of aerosols in the Mexico City Metropolitan Area, Atmos. Chem. Phys., 8, 6665–6679, doi:10.5194/acp-8-6665-2008, 2008.

Birch, M. E. and Cary, R. A.: Elemental carbon-based method for monitoring occupational exposures to particulate diesel exhaust, Aerosol Sci. Technol., 25, 221–241, 1996.

Bond, T. C. and Bergstrom, R. W.: Light absorption by carbonaceous particles: an investigative review, Aerosol Sci. Technol., 40, 27–67, doi:10.1080/02786820500421521, 2006.

Bond, T. C., Anderson, T. L., and Campbell, D.: Calibration and intercomparison of filter-based measurements of visible light absorption by aerosols, Aerosol Sci. Tech., 30, 582–600, 1999.

Brunekreef, B., Janssen, N. A., de Hartog, J., Harssema, H., Knape, M., and van Vliet, P.: Air pollution from truck traffic and lung function in children living near motorways, Epidemiology, 8, 298–303, 1997.

Carslaw, D. C.: The openair manual – open-source tools for analysing air pollution data, Manual for version 0.7-0, King's College, London, 2012.

Carslaw, D. C. and Ropkins, K.: Openair – an R package for air quality data analysis, Environ. Modell. Softw., 27–28, 52–61, 2012.

Cavalli, F., Viana, M., Yttri, K. E., Genberg, J., and Putaud, J.-P.: Toward a standardised thermal-optical protocol for measuring atmospheric organic and elemental carbon: the EUSAAR protocol, Atmos. Meas. Tech., 3, 79–89, doi:10.5194/amt-3-79-2010, 2010.

Chow, J. C., Watson, J. G., Pritchett, L. C., Pierson, W. R., Frazier, C. A., and Purcell, R. G.: The DRI thermal optical reflectance carbon analysis system – description, evaluation and applications in United-States air-quality studies, Atmos. Environ., 27, 1185–1201, 1993.

Chow, J. C., Watson, J. G., Crow, D., Lowenthal, D. H., and Merrifield, T.: Comparison of IMPROVE and NIOSH carbon measurements, Aerosol Sci. Technol., 34, 23–34, 2001.

Chow, J. C., Watson, J. G., Chen, L. W., Arnott, W. P., Moosmuller, H., and Fung, K.: Equivalence of elemental carbon by thermal/optical reflectance and transmittance with different temperature protocols, Environ. Sci. Technol., 38, 4414–4422, 2004.

Chow, J. C., Watson, J. G., Doraiswamy, P., Chen, L.-W. A., Sodeman, D. A., Lowenthal, D. H., Park, K., Arnott, W. P., and Motallebi, N.: Aerosol light absorption, black carbon, and elemental carbon at the Fresno Supersite, California, Atmos. Res., 93, 874–887, 2009.

Chow, J. C., Watson, J. G., Chen, L.-W. A., Rice, J., and Frank, N. H.: Quantification of $PM_{2.5}$ organic carbon sampling artifacts in US networks, Atmos. Chem. Phys., 10, 5223–5239, doi:10.5194/acp-10-5223-2010, 2010.

Conny, J. M., Klinedinst, D. B., Wight, S. A., and Paulsen, J. L.: Optimizing thermal-optical methods for measuring atmospheric elemental (black) carbon: a response surface study, Aerosol Sci. Technol., 37, 703–723, 2003.

Fernández-Camacho, R., Rodríguez, S., de la Rosa, J., Sánchez de la Campa, A. M., Viana, M., Alastuey, A., and Querol, X.: Ultrafine particle formation in the inland sea breeze airflow in Southwest Europe, Atmos. Chem. Phys., 10, 9615–9630, doi:10.5194/acp-10-9615-2010, 2010.

Fuzzi, S., Andreae, M. O., Huebert, B. J., Kulmala, M., Bond, T. C., Boy, M., Doherty, S. J., Guenther, A., Kanakidou, M., Kawamura, K., Kerminen, V.-M., Lohmann, U., Russell, L. M., and Pöschl, U.: Critical assessment of the current state of scientific knowledge, terminology, and research needs concerning the role of organic aerosols in the atmosphere, climate, and global change, Atmos. Chem. Phys., 6, 2017–2038, doi:10.5194/acp-6-2017-2006, 2006.

GAW/WMO: Position of the GAW Scientific Advisory Group on the use of Black Carbon terminology, GAW/WMO SAG – AEROSOL, 2011.

Grivas, G., Cheristanidis, S., and Chaloulakou, A.: Elemental and organic carbon in the urban environment of Athens. Seasonal and diurnal variations and estimates of secondary organic carbon, Sci. Total Environ., 414, 535–545, 2012.

Hansen, A. D. A., Rosen, H., and Novakov, T.: The aethalometer-an instrument or the realtime measurement of optical absorption by aerosol particles, Sci. Total Environ., 36, 191–196, 1984.

He, X., Li, C. C., Lau, A. K. H., Deng, Z. Z., Mao, J. T., Wang, M. H., and Liu, X. Y.: An intensive study of aerosol optical properties in Beijing urban area, Atmos. Chem. Phys., 9, 8903–8915, doi:10.5194/acp-9-8903-2009, 2009.

Hollander, M. and Wolfe, D. A.: Nonparametric Statistical Methods, 2nd Edn., New York, John Wiley & Sons, 421–423, 1999.

Jimenez, J. L., Canagaratna, M. R., Donahue, N. M., Prevot, A. S. H., Zhang, Q., Kroll, J. H., DeCarlo, P. F., Allan, J. D., Coe, H., Ng, N. L., Aiken, A. C., Docherty, K. S., Ulbrich, I. M., Grieshop, A. P., Robinson, A. L., Duplissy, J., Smith, J. D., Wilson, K. R., Lanz, V. A., Hueglin, C., Sun, Y. L., Tian, J., Laaksonen, A., Raatikainen, T., Rautiainen, J., Vaattovaara, P., Ehn, M., Kulmala, M., Tomlinson, J. M., Collins, D. R., Cubison, M. J., Dunlea, E. J., Huffman, J. A., Onasch, T. B., Alfarra, M. R., Williams, P. I., Bower, K., Kondo, Y., Schneider, J., Drewnick, F., Borrmann, S., Weimer, S., Demerjian, K., Salcedo, D., Cottrell, L., Griffin, R., Takami, A., Miyoshi, T., Hatakeyama, S., Shimono, A., Sun, J. Y., Zhang, Y. M., Dzepina, K., Kimmel, J. R., Sueper, D., Jayne, J. T., Herndon, S. C., Trimborn, A. M., Williams, L. R., Wood, E. C., Middlebrook, A. M., Kolb, C. E., Baltensperger, U., and Worsnop, D. R.: Evolution of organic aerosols in the atmosphere, Science, 326, 1525–1529, 2009.

Kanakidou, M., Seinfeld, J. H., Pandis, S. N., Barnes, I., Dentener, F. J., Facchini, M. C., Van Dingenen, R., Ervens, B., Nenes, A., Nielsen, C. J., Swietlicki, E., Putaud, J. P., Balkanski, Y., Fuzzi, S., Horth, J., Moortgat, G. K., Winterhalter, R., Myhre, C. E. L., Tsigaridis, K., Vignati, E., Stephanou, E. G., and Wilson, J.: Organic aerosol and global climate modelling: a review, Atmos. Chem. Phys., 5, 1053–1123, doi:10.5194/acp-5-1053-2005, 2005.

Karanasiou, A., Diapouli, E., Cavalli, F., Eleftheriadis, K., Viana, M., Alastuey, A., Querol, X., and Reche, C.: On the quantification of atmospheric carbonate carbon by thermal/optical analysis protocols, Atmos. Meas. Tech., 4, 2409–2419, doi:10.5194/amt-4-2409-2011, 2011.

Koulouri, E., Saarikoski, S., Theodosi, C., Markaki, Z., Gerasopoulos, E., Kouvarakis, G., Mäkelä, T., Hillamo, R., and Mihalopoulos, N.: Chemical composition and sources of fine and coarse aerosol particles in the Eastern Mediterranean, Atmos. Environ., 42, 6542–6550, 2008.

Mader, B. T., Flagan, R. C., and Seinfeld, J. H.: Sampling atmospheric carbonaceous aerosols using a particle trap impactor/denuder sampler, Environ. Sc. Technol., 35, 4857–4867, 2001.

Maenhaut, W., Cafmeyer, J., Chi, X., and Schwarz, J.: Assessment of artefacts in filter collections for carbonaceous aerosols and the particulate mass, J. Aerosol Sci., 32, S673–S674, 2001.

Maenhaut, W., Claeys, M., Vercauteren, J., and Roekens, E.: Comparison of different operational parameters for thermal-optical EC/OC measurements of filter samples from Flanders, Belgium, European Aerosol Conference 2012 abstracts, available at: http://www.eac2012.com/EAC2012Book/files/235.pdf, 2012.

Mauderly, J. L. and Chow, J. C.: Health effects of organic aerosols, Inhal. Toxicol., 20, 257–288, 2008.

Minguillón, M. C., Perron, N., Querol, X., Szidat, S., Fahrni, S. M., Alastuey, A., Jimenez, J. L., Mohr, C., Ortega, A. M., Day, D. A., Lanz, V. A., Wacker, L., Reche, C., Cusack, M., Amato, F., Kiss, G., Hoffer, A., Decesari, S., Moretti, F., Hillamo, R., Teinilä, K., Seco, R., Peñuelas, J., Metzger, A., Schallhart, S., Müller, M., Hansel, A., Burkhart, J. F., Baltensperger, U., and Prévôt, A. S. H.: Fossil versus contemporary sources of fine elemental and organic carbonaceous particulate matter during the DAURE campaign in Northeast Spain, Atmos. Chem. Phys., 11, 12067–12084, doi:10.5194/acp-11-12067-2011, 2011.

Mohr, C., DeCarlo, P. F., Heringa, M. F., Chirico, R., Slowik, J. G., Richter, R., Reche, C., Alastuey, A., Querol, X., Seco, R., Peñuelas, J., Jiménez, J. L., Crippa, M., Zimmermann, R., Baltensperger, U., and Prévôt, A. S. H.: Identification and quantification of organic aerosol from cooking and other sources in Barcelona using aerosol mass spectrometer data, Atmos. Chem. Phys., 12, 1649–1665, doi:10.5194/acp-12-1649-2012, 2012.

Müller, T., Henzing, J. S., de Leeuw, G., Wiedensohler, A., Alastuey, A., Angelov, H., Bizjak, M., Collaud Coen, M., Engström, J. E., Gruening, C., Hillamo, R., Hoffer, A., Imre, K., Ivanow, P., Jennings, G., Sun, J. Y., Kalivitis, N., Karlsson, H., Komppula, M., Laj, P., Li, S.-M., Lunder, C., Marinoni, A., Martins dos Santos, S., Moerman, M., Nowak, A., Ogren, J. A., Petzold, A., Pichon, J. M., Rodriquez, S., Sharma, S., Sheridan, P. J., Teinilä, K., Tuch, T., Viana, M., Virkkula, A., Weingartner, E., Wilhelm, R., and Wang, Y. Q.: Characterization and intercomparison of aerosol absorption photometers: result of two intercomparison workshops, Atmos. Meas. Tech., 4, 245–268, doi:10.5194/amt-4-245-2011, 2011.

Novakov, T., Andreae, M. O., Gabriel, R., Kirchstetter, T. W., Mayol-Bracero, O. L., and Ramanathan, V.: Origin of carbonaceous aerosols over the tropical Indian Ocean: biomass burning or fossil fuels?, Geophys. Res. Lett., 27, 4061–4064, 2000.

Pérez, N., Pey, J., Querol, X., Alastuey, A., López, J. M., Viana, M.: Partitioning of major and trace components in PM_{10}-$PM_{2.5}$-PM_1 at an urban site in Southern Europe, Atmos. Environ., 42, 1677–1691, 2008.

Petzold, A. and Schönlinner, M.: Multi-angle absorption photometry – a new method for the measurement of aerosol light absorption and atmospheric black carbon, J. Aerosol Sci., 35, 421–441, 2004.

Pey, J., Pérez, N., Querol, X., Alastuey, A., Cusack, M., and Reche, C.: Intense winter atmospheric pollution episodes affecting the Western Mediterranean, Sci. Total Environ., 408, 1951–1959, 2010.

Phuah, C. H., Peterson, M. R., Richards, M. H., Turner, J. H., and Dillner, A. M.: A temperature calibration procedure for the sunset laboratory carbon aerosol analysis lab instrument, Aerosol Sci. Tech., 43, 1013–1021, 2009.

Pio, C. A., Castro, L. M., and Ramos, M. O.: Differentiated determination of organic and elemental carbon in atmospheric aerosol particles by thermal.optics method, in: Proceedings of the Sixth European Symposium: Physico-Chemical Behaviour of Atmospheric Pollutants, edited by: Angeletti, G. and Restelli, G., Report EUR 15609/2 EN, European Commission, 706–711, 1994.

Pio, C. A., Legrand, M., Oliveira, T., Afonso, J., Santos, C., Caseiro, A., Fialho, P., Barata, F., Puxbaum, H., Sanchez-Ochoa, A., Kasper-Giebl, A., Gelencsér, A., Preunkert, S., and Schock, M.: Climatology of aerosol composition (organic versus inorganic) at nonurban sites on a west-east transect across Europe, J. Geophys. Res., 112, D23S02, doi:10.1029/2006JD008038, 2007.

Pio, C. A., Cerqueira, M., Harrison, R. M., Nunes, T., Mirante, F., Alves, C., Oliveira, C., Sanchez de la Campa, A., Artiñano, B., and Matos, M.: OC/EC Ratio Observations in Europe: re-thinking the approach for apportionment between primary and secondary organic carbon, Atmos. Environ., 45, 6121–6132, 2011.

Plaza, J., Artíñano, B., Salvador, P., Gómez-Moreno, F. J., Pujadas, M., and Pio, C. A.: Short-term SOA estimations with a modified OC/EC primary ratio method at a suburban site in Madrid (Spain), Atmos. Environ., 45, 2496–2506, 2011.

Putaud, J.-P., Van Dingenen, R., Alastuey, A., Bauer, H., Birmili, W., Cyrys, J., Flentje, H., Fuzzi, S., Gehrig, R., Hansson, H. C., Harrison, R. M., Herrmann, H., Hitzenberger, R., Hüglin, C., Jones, A. M., Kasper-Giebl, A., Kiss, G., Kousa, A., Kuhlbusch, T. A. J., Löschau, G., Maenhaut, W., Molnar, A., Moreno, T., Pekkanen, J., Perrino, C., Pitz, M., Puxbaum, H., Querol, X., Rodriguez, S., Salma, I., Schwarz, J., Smolik, J., Schneider, J., Spindler, G., ten Brink, H., Tursic, J., Viana, M., Wiedensohler, A., and Raes, F.: A European aerosol phenomenology – 3: Physical and chemical characteristics of particulate matter from 60 rural, urban, and kerbside sites across Europe, Atmos. Environ., 44, 1308–1320, 2010.

Querol, X., Alastuey, A., Moreno, T., Viana, M. M., Castillo, S., Pey, J., Rodríguez, S., Artiñano, B., Salvador, P., Sánchez, M., Garcia Dos Santos, S., Herce Garraleta, M. D., Fernandez-Patier, R., Moreno-Grau, S., Minguillón, M. C., Monfort, E., Sanz, M. J., Palomo-Marín, R., Pinilla-Gil, E., Cuevas, E., De la Rosa, J., and Sanchez de la Campa, A.: Spatial and temporal variations in airborne particulate matter (PM_{10} and $PM_{2.5}$) across Spain 1999–2005, Atmos. Environ., 42, 3964–3979, 2008.

Ramana, M. V., Ramanathan, V., Feng, Y., Yoon, S. C., Kim, S. W., Carmichael, G. R., and Schauer, J. J.: Warming influenced by the ratio of black carbon to sulphate and the black-carbon source, Nature Geosci., 3, 542–545, 2010.

Ramanathan, V. and Carmichael, G.: Global and regional climate changes due to black carbon, Nature Geosci., 1, 221–227, 2008.

Reche, C., Querol, X., Alastuey, A., Viana, M., Pey, J., Moreno, T., Rodríguez, S., González, Y., Fernández-Camacho, R., de la Rosa, J., Dall'Osto, M., Prévôt, A. S. H., Hueglin, C., Harrison, R. M., and Quincey, P.: New considerations for PM, Black Carbon and particle number concentration for air quality monitoring across different European cities, Atmos. Chem. Phys., 11, 6207–6227, doi:10.5194/acp-11-6207-2011, 2011.

Salmi, T., Määttä, A., Anttila, P., Ruoho-Airola, T., and Amnell, T.: Detecting trends of annual values of atmospheric pollutants by the Mann–Kendall test and Sen's slope estimates –

the Excel template application MAKESENS, in: Publications on Air Quality No. 31, editd by: Finnish Meteorological Institute, p. 35, Finnish Meteorological Institute, 2002.

Schauer, J. J., Mader, B. T., Deminter, J. T., Heidemann, G., Bae, M. S., Seinfeld, J. H., Flagan, R. C., Cary, R. A., Smith, D., Huebert, B. J., Bertram, T., Howell, S., Kline, J. T., Quinn, P., Bates, T., Turpin, B., Lim, H. J., Yu, J. Z., Yang, H., and Keywood, M. D.: ACE-Asia intercomparison of a thermal-optical method for the determination of particle phase organic and elemental carbon, Environ. Sci. Technol., 37, 993–1001, 2003.

Schmid, H., Laskus, L., Abraham, H. J., Baltensperger, U., Lavanchy, V., Bizjak, M., Burba, P., Cachierv, H., Crow, D., Chow, J., Gnauk, T., ten Brink, H. M., Giesen, K.-P., Hitzenberger, R., Hueglin, C., Maenhaut, W., Pio, C., Carvalho, A., Putaud, J. P., Toom-Sauntry, D., and Puxbaum, H.: Results of the 19 “carbon conference” international aerosol carbon round robin test stage I, Atmos. Environ., 20, 2111–2121, 2001.

Seco, R., Peñuelas, J., Filella, I., Llusià, J., Molowny-Horas, R., Schallhart, S., Metzger, A., Müller, M., and Hansel, A.: Contrasting winter and summer VOC mixing ratios at a forest site in the Western Mediterranean Basin: the effect of local biogenic emissions, Atmos. Chem. Phys., 11, 13161–13179, doi:10.5194/acp-11-13161-2011, 2011.

Sen, P. K.: Estimates of regression coefficient based on kendall’s tau, J. Am. Stat. Assoc., 63, 1379–1389, 1968.

Shindell, D., Kuylenstierna, J. C. I., Vignati, E., van Dingenen, R., Amann, M., Klimont, Z., Anenberg, S. C., Muller, N., Janssens-Maenhout, G., Raes, F., Schwartz, J., Faluvegi, G., Pozzoli, L., Kupiainen, K., Höglund-Isaksson, L., Emberson, L., Streets, D., Ramanathan, V., Hicks, K., Oanh, N. T. K., Milly, G., Williams, M. L., Demkine, V., and Fowler, D.: Simultaneously mitigating near-term climate change and improving human health and food security, Science, 335, 183–189, doi:10.1126/science.1210026, 2012.

Spindler, G., Brüggemann, E., Gnauk, T., Grüner, A., Müller, K., and Herrmann, H.: A four-year size-segregated characterization study of particles PM_{10}, $PM_{2.5}$ and PM_1 depending on air mass origin at Melpitz, Atmos. Environ., 44, 164–173, 2010.

Subramanian, R., Khlystov, A. Y., Cabada, J. C., and Robinson, A. L.: Positive and negative artifacts in particulate organic carbon measurements with denuded and undenuded sampler configurations, Aerosol Sci. Technol., 38, 27–48, 2004.

Subramanian, R., Khlystov, A. Y., and Robinson, A. L.: Effect of peak inert-mode temperature on elemental carbon measured using thermal optical analysis. Aerosol Sci. Technol., 40, 763–780, 2006.

Szidat, S., Prevot, A. S. H., Sandradewi, J., Alfarra, M. R., Synal, H. A., Wacker, L., and Baltensperger, U.: Dominant impact of residential wood burning on particulate matter in Alpine valleys during winter, Geophys. Res. Lett., 34, L05820, doi:10.1029/2006GL028325, 2007.

Theil, H.: A rank invariant method of linear and polynomial regression analysis, i, ii, iii, P. K. Ned. Akad. A Math., 53, 386–392, 1950.

Turpin, B. J., Saxena, P., and Andrews, E.: Measuring and simulating particulate organics in the atmosphere: problems and prospects, Atmos. Environ., 34, 2983–3013, 2000.

Verma, V., Ning, Z., Cho, A. K., Schauer, J. J., Shafer, M. M., and Sioutas, C.: Redox activity of urban quasi-ultrafine particles from primary and secondary sources, Atmos. Environ., 43, 6360–6368, 2009.

Viana, M., Chi, X., Maenhaut, W., Querol, X., Alastuey, A., Mikuska, P., and Vecera, Z.: Organic and elemental carbon concentrations in carbonaceous aerosols during summer and winter sampling campaigns in Barcelona, Spain, Atmos. Environ., 40, 2180–2193, 2006.

Viana, M., Maenhaut, W., ten Brink, H. M., Chi, X., Weijers, X., Querol, X., Alastuey, X., Mikuska, P., and Vecera, Z.: Comparative analysis of organic and elemental carbon concentrations in carbonaceous aerosols in three European cities, Atmos. Environ., 41, 5972–598, 2007.

Viana, M., Querol, X., Reche, C., Favez, O., Malherbe, L., Ustache, A., Bartonova, A., Liu, H.-Y., and Guerreiro, C.: Particle number (PNC) and black carbon (BC) in EU urban air quality networks, ETC/ACM Technical Paper 2012/6, 2013.

Wang, Y., Chung, A., and Paulson, S. E.: The effect of metal salts on quantification of elemental and organic carbon in diesel exhaust particles using thermal-optical evolved gas analysis, Atmos. Chem. Phys., 10, 11447–11457, doi:10.5194/acp-10-11447-2010, 2010.

WHO: Health Effects of Black Carbon, edited by: Janssen, N. A. H., Gerlofs-Nijland, M. E., Lanki, T., Salonen, R. O., Cassee, F., Hoek, G., Fischer, P., Brunekreef, B., Krzyzanowski, WHO's Regional Office for Europe, Copenhaguen, 86 pp., ISBN 978-9-28900265-3, available at: http://www.euro.who.int/__data/assets/pdf_file/0004/162535/e96541.pdf, 2012.

WHO: Review of evidence on health aspects of air pollution – REVIHAAP. First Results. WHO's Regional Office for Europe, Copenhaguen, 28 pp., available at: http://www.euro.who.int/__data/assets/pdf_file/0020/182432/e96762-final.pdf, 2013.

Williams, M. L. and Carslaw, D. C.: New directions: science and policy – out of step on NO_x and NO_2?, Atmos. Environ., 45, 3911–3912, 2011.

Yttri, K. E., Aas, W., Bjerke, A., Cape, J. N., Cavalli, F., Ceburnis, D., Dye, C., Emblico, L., Facchini, M. C., Forster, C., Hanssen, J. E., Hansson, H. C., Jennings, S. G., Maenhaut, W., Putaud, J. P., and Tørseth, K.: Elemental and organic carbon in PM_{10}: a one year measurement campaign within the European Monitoring and Evaluation Programme EMEP, Atmos. Chem. Phys., 7, 5711–5725, doi:10.5194/acp-7-5711-2007, 2007.

Table 1. List of monitoring sites providing data for nmC, OC and EC and EBC (µg m^{-3}) used in this study and information on PM_x, location, type of environment represented and study period. *N*: number of samples.

Location	Code	PM_x	Province	Longitude	Latitude	Altitude (m a.s.l.)	Type of site	Study period	*N* nmC	nmC	*N* OC/EC	OC	EC	EBC
Izaña	IZO	$PM_{2.5}$	Tenerife	16°30′35″ W	28°18′00″ N	2390	Remote	2006–2007	99	1.2	35	1.15	0.07	
Montsec	MSC	$PM_{2.5}$	Lleida	00°43′46″ E	42°03′06″ N	1600	Remote	2009-2010		1.7	280	1.60	0.13	0.18
Bemantes	BEM	$PM_{2.5}$	A Coruña	08°10′50″ W	43°20′15″ N	170	Rural	2001	45	3.8				
Campillos	CAM	$PM_{2.5}$	Málaga	04°51′41″ W	37°02′44″ N	460	Rural	2010	42	1.8				
El Perdón	PER	PM_{10}	Navarra	01°47′00″ W	42°44′00″ N	900	Rural	2003	55	2.4				
Endrinal Cortijo	END	PM_{10}	Badajoz	06°19′34″ W	38°29′09″ N	490	Rural	2006–2007	60	2.2				
Matalascañas	MAT	$PM_{2.5}$	Huelva	06°34′11″ W	37°00′59″ N	10	Rural	2010	73	2.5				
San Jorge	SJO	PM_{10}	Badajoz	06°22′25″ W	38°30′00″ N	560	Rural	2008	15	2.6	15	2.28	0.28	
Valverde del Camino	VALV	$PM_{2.5}$	Huelva	06°45′21″ W	37°34′47″ N	220	Rural	2007–2010	85	2.5				
Monagrega	MON	PM_{10}	Teruel	00°19′15″ W	40°56′23″ N	600	Rural	1999–2000	112	2.3	15	2.20	0.20	
Montseny	MSY	$PM_{2.5}$	Barcelona	02°22′40″ E	41°46′47″ N	730	Rural	2002–2010	255	2.4	425	2.01	0.22	0.46
Can Llompart	CLL	PM_{10}	Mallorca	03°02′32″ E	39°50′41″ N	25	Rural	2010–2011	163	2.0		1.91	0.20	
Arenosillo	ARE	$PM_{2.5}$	Huelva	06°44′03″ W	37°06′14″ N	44	Indust.-Suburban	2007–2008	43	4.6	21	2.99	0.64	
Alacant	ALA	PM_{10}	Alacant	00°30′57″ W	38°23′14″ N	120	Indust.-Suburban	2004–2006		3.5				
Monzón	MOZ	$PM_{2.5}$	Huesca	00°11′31″ W	41°54′55″ N	272	Indust.-Suburban	2011		4.4	51	3.82	0.54	
Onda	OND	PM_{10}	Castelló	00°15′09″ W	39°57′44″ N	163	Indust.-Suburban	2000–2007	317	3.7	137	3.03	0.44	
Plaza Castillo	PCAS	PM_{10}	Almería	01°53′42″ W	36°59′48″ N	23	Indust.-Suburban	2008–2010	94	2.3				
Poblado	POB	PM_{10}	Córdoba	04°55′36″ W	38°06′36″ N	460	Indust.-Suburban	2010	26	3.5				
Ponferrada	PFE	$PM_{2.5}$	León	06°35′05″ W	42°32′34″ N	541	Indust.-Suburban	2007–2008	99	4.1	51	3.88	0.54	
Punta Umbría	PUM	$PM_{2.5}$	Huelva	06°57′46″ W	37°11′13″ N	3	Indust.-Suburban	2007–2010	98	3.9				
Santa Cruz	STC	$PM_{2.5}$	Tenerife	16°14′51″ W	28°28′21″ N	52	Indust.-Suburban	2002–2009	233	1.8	77	0.91	0.94	1.40
Torrelavega	TORR	PM_{10}	Cantabria	04°03′51″ W	43°20′47″ N	20	Indust.-Suburban	2007–2008	79	3.7				
Agost	AGO	PM_{10}	Alacant	00°38′17″ W	38°26′11″ N	312	Industrial-Urban	2006–2008	81	4.6				
Alcalá de Guadaira	AGUAD	$PM_{2.5}$	Sevilla	05°50′00″ W	37°20′31″ N	60	Industrial-Urban	2007–2010	70	3.9				
Almassora	ALM	$PM_{2.5}$	Castelló	00°03′23″ W	39°56′43″ N	27	Industrial-Urban	2005	10	3.5				
Alsasua	ALS	PM_{10}	Navarra	02°10′00″ W	42°54′00″ N	534	Industrial-Urban	2002–2003	94	5.7				
Avilés	AVI	$PM_{2.5}$	Asturias	05°55′34″ W	43°33′36″ N	14	Industrial-Urban	2011		6.9	85	3.92	2.93	
Bailén	BAIL	$PM_{2.5}$	Jaén	03°47′02″ W	38°05′34″ N	337	Industrial-Urban	2004–2010	67	10.6	34	5.39	3.12	
Bajo Cadagua	BCAD	PM_{10}	Vizcaya	02°58′25″ W	43°15′30″ N	60	Industrial-Urban	2010		6.4	21	4.68	1.71	
Borriana	BOR	PM_{10}	Castelló	00°05′10″ W	39°53′38″ N	20	Industrial-Urban	2004–2007	148	5.8	91	3.27	0.80	
Huelva-Campus Univ.	HUE	$PM_{2.5}$	Huelva	05°55′29″ W	37°16′17″ N	17	Industrial-Urban	2000–2010	246	4.2	96	2.42	0.87	1.31
L'Alcora	L'AL	PM_{10}	Castelló	00°12′43″ W	40°04′07″ N	175	Industrial-Urban	2002–2005	329	3.9	156	3.18	0.84	
La Línea	LLI	$PM_{2.5}$	Cádiz	05°20′49″ W	36°09′37″ N	1	Industrial-Urban	2005–2010		4.0	47	2.26	0.99	
Llodio	LLO	$PM_{2.5}$	Alava	02°57′44″ W	43°08′42″ N	122	Industrial-Urban	2001	44	6.9				
Los Barrios	LBARR	$PM_{2.5}$	Cádiz	05°28′55″ W	36°11′02″ N	45	Industrial-Urban	2007–2010	139	3.3				
Montcada	MONT	PM_{10}	Barcelona	02°11′00″ E	41°28′00″ N	38	Industrial-Urban	2010		6.4	58	4.49	1.87	
Puente Mayorga	PMAY	PM_{10}	Campo Gib	05°23′12″ W	36°11′00″ N	15	Industrial-Urban	2007–2010	169	4.2				
Puertollano	PUER	$PM_{2.5}$	Ciudad Real	04°05′19″ W	38°41′64″ N	670	Industrial-Urban	2004	98	6.9				
Tarragona	TAR	$PM_{2.5}$	Tarragona	01°14′52″ E	41°07′29″ N	20	Industrial-Urban	2001	43	6.4				
Torredonjimeno	TDJ	$PM_{2.5}$	Jaén	03°56′46″ W	37°45′49″ N	605	Industrial-Urban	2007–2010	88	5.0				
Vila-real	VIL	PM_{10}	Castelló	00°06′21″ W	39°56′30″ N	60	Industrial-Urban	2002–2006	347	5.2				
Zabalgarbi	ZAB	PM_{10}	Vizcaya	02°58′13″ W	43°16′03″ N	119	Industrial-Urban	2011		6.0	14	3.65	2.30	

Title Page
Abstract | Introduction
Conclusions | References
Tables | Figures
◀| |▶
◀ ▶
Back | Close
Full Screen / Esc
Printer-friendly Version
Interactive Discussion

Table 1. Continued.

Location	Code	PM_x	Province	Longitude	Latitude	Altitude (m a.s.l.)	Type of site	Study period	*N* nmC	nmC	*N* OC/EC	OC	EC	EBC
Badajoz	BAD	$PM_{2.5}$	Badajoz	06°34′48″ W	38°31′48″ N	188	Suburban	2004–2005	95	4.1				
Burgos	BUR	$PM_{2.5}$	Burgos	03°38′15″ W	42°20′06″ N	889	Suburban	2004	85	4.5				
Cartagena-Santa Ana	STAA	$PM_{2.5}$	Murcia	01°00′40″ W	37°39′10″ N	15	Suburban	2004	83	3.0				
Palma de Mallorca	PMM	$PM_{2.5}$	Mallorca	02°35′24″ E	39°35′24″ N	117	Suburban	2004	103	3.3				
Nerva	NER	PM_{10}	Huelva	06°33′25″ W	37°41′75″ N	336	Suburban	2010	90	4.5				
El Vacar	VAC	PM_{10}	Córdoba	04°50′47″ W	38°04′35″ N	605	Suburban-Rural	2010	34	4.3				
Chapineria	CHA	$PM_{2.5}$	Madrid	04°12′15″ W	40°22′45″ N	675	Suburban-Rural	2004	96	3.9				
Albacete	ALB_UB	$PM_{2.5}$	Albacete	01°57′07″ W	38°58′45″ N	686	Urban	2011		3.7	88	3.3	.65	
Alcobendas	ALC_UB	$PM_{2.5}$	Madrid	03°37′39″ W	40°32′42″ N	667	Urban	2001	34	9.3				
Barcelona-CSIC	BCN_UB	$PM_{2.5}$	Barcelona	02°07′09″ E	41°23′05″ N	68	Urban	2003–2011	405	5.6	474	3.05	1.51	2.06
Bilbao P Europa	BIL_UB	$PM_{2.5}$	Bilbao	02°54′08″ W	43°15′18″ N	19	Urban	2009		2.6	30	1.80	0.80	
Girona-Urban	GIR_UB	$PM_{2.5}$	Girona	02°48′37″ E	41°59′30″ N	76	Urban	2009	82	6.2				
Granada University	GRA_UB	PM_{10}	Granada	03°34′48″ W	37°10′48″ N	680	Urban	2006–2010	100	6.0	96	4.46	1.51	2.62
Lepanto	CORD_UB	$PM_{2.5}$	Córdoba	04°46′06″ W	37°53′39″ N	108	Urban	2007–2010	98	4.6				
Madrid (CIEMAT)	MAD_UB	$PM_{2.5}$	Madrid	03°42′19″ W	40°25′05″ N	680	Urban	2006–2007[b]		5.1	584	3.80	1.32	
Melilla	MEL_UB	$PM_{2.5}$	Melilla	02°56′30″ W	35°17′40″ N	10	Urban	2007	97	4.6	51	3.85	1.33	
Moguer	MOG_UB	PM_{10}	Huelva	06°50′01″ W	37°16′54″ N	10	Urban	2008–2010	119	4.8				
Pamplona[a]	PAM_UB	$PM_{2.5}$	Navarra	01°38′60″ W	42°49′00″ N	449	Urban	2009[a]	80	4.0				
Príncipes	SEV_UB	$PM_{2.5}$	Sevilla	06°00′15″ W	37°22′36″ N	8	Urban	2007–2010	98	4.8				
Ronda del Valle	JAE_UB	$PM_{2.5}$	Jaén	03°46′51″ W	37°47′01″ N	480	Urban	2007–2010	91	4.8				
Sabadell P Central	SAB_UB	$PM_{2.5}$	Barcelona	02°06′34″ E	41°31′22″ N	180	Urban	2007		5.8	41	4.11	1.67	
San Fernando	CAD_UB	$PM_{2.5}$	Cádiz	06°12′06″ W	36°27′43″ N	35	Urban	2007–2010	88	3.0				
Santander	SAN_UB	$PM_{2.5}$	Cantabria	03°47′25″ W	43°28′04″ N	30	Urban	2007–2008	101	3.6	51	3.24	0.82	
Zaragoza	ZAR_UB	$PM_{2.5}$	Zaragoza	00°52′18″ W	41°40′08″ N	195	Urban	2011		4.6	67	3.57	1.6	
Las Palmas	LPM_UB	$PM_{2.5}$	Gran Canaria	15°24′49″ W	28°08′04″ N	20	Urban	2001	47	6.6				
Barreda-Torrelavega	BARR_T	$PM_{2.5}$	Cantabria	04°02′34″ W	43°22′03″ N	18	Traffic-Industrial	2009	79	4.6	43	3.79	1.43	
Almería Mediterráneo	ALM_T	$PM_{2.5}$	Almería	02°27′25″ W	36°50′42″ N	51	Traffic-Urban	2007–2010	84	4.5				
Barcelona-Sagrera	BCN_T	$PM_{2.5}$	Barcelona	02°11′22″ E	41°25′21″ N	24	Traffic-Urban	2000–2001	108	10.3				
Pamplona-Traffic[a]	PAM_T	$PM_{2.5}$	Navarra	01°38′60″ W	42°49′00″ N	449	Traffic-Urban	2009[a]	77	5.0				
Bilbao-Salud	BIL_T	$PM_{2.5}$	Vizcaya	02°56′45″ W	43°15′08″ N	19	Traffic-Urban	2009		5.7	20	3.58	2.16	
Carranque	MAL_T	$PM_{2.5}$	Málaga	04°25′46″ W	36°43′13″ N	36	Traffic-Urban	2007–2010	94	4.4				
Cartagena-Bastarreche	CAR_T	PM_{10}	Murcia	00°58′28″ W	37°36′14″ N	20	Traffic-Urban	2004	98	10.1				
Girona-Traffic	GIR_T	$PM_{2.5}$	Girona	02°49′31″ E	41°58′69″ N	76	Traffic-Urban	2009	87	9.5				
Granada Norte	GRA_T	$PM_{2.5}$	Granada	03°36′28″ W	37°11′51″ N	689	Traffic-Urban	2007–2010	72	5.9				
Madrid (Esc. Aguirre)	MAD_T	$PM_{2.5}$	Madrid	03°40′52″ W	40°25′32″ N	672	Traffic-Urban	2011		8.3	75	4.19	4.13	
Sabadell-Gran Vía	SAB_T	$PM_{2.5}$	Barcelona	02°06′05″ E	41°33′40″ N	180	Traffic-Urban	2007		8.6	28	5.43	3.16	

[a] Aldabe et al. (2011).

[b] Plaza et al. (2011).

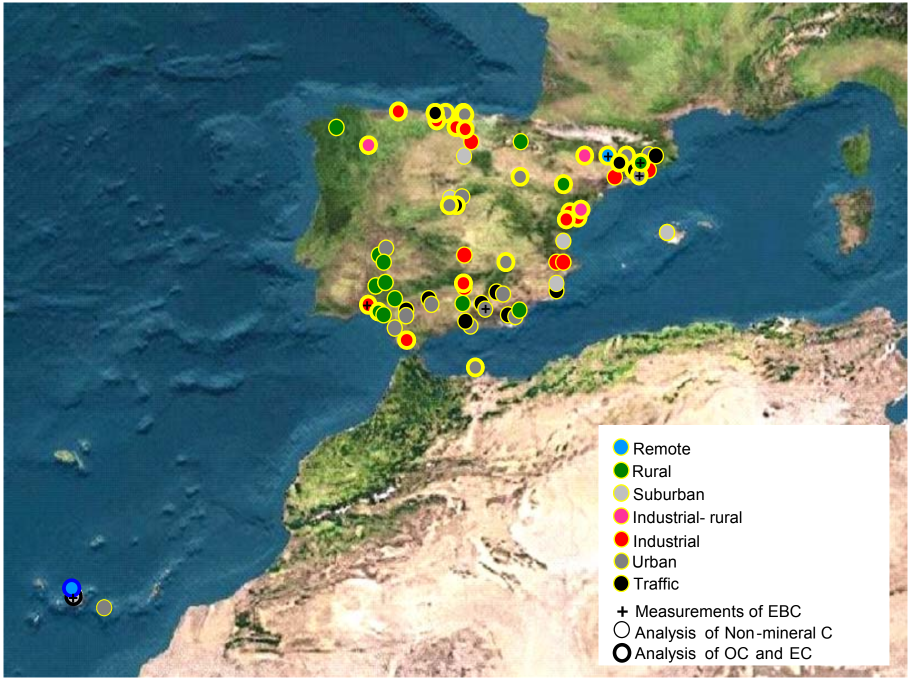

Fig. 1. Location of the monitoring stations across mainland Spain, the Balearic and Canary Archipelagoes and the Spanish Northern African territories from where during the period 1999–2011 data on nmC, OC-EC and EBC were obtained.

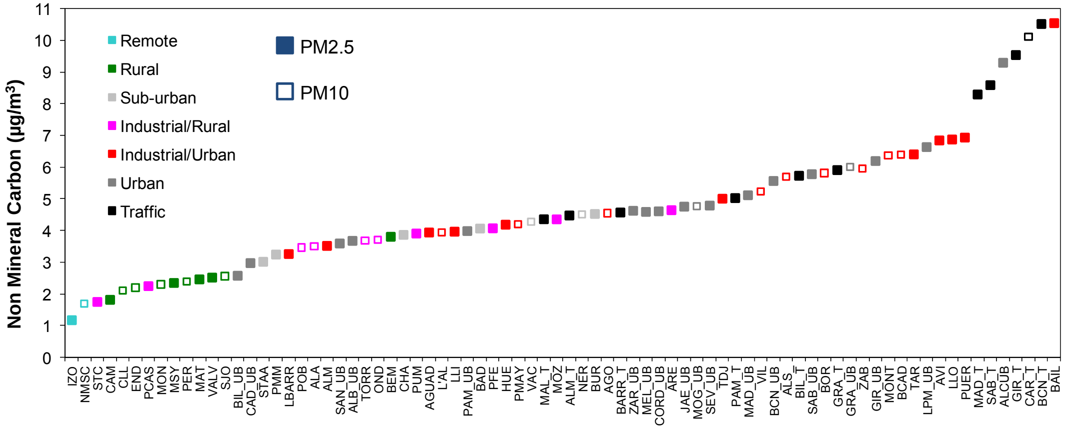

Fig. 2. Mean nmC concentrations in $PM_{2.5}$ (solid) and PM_{10} (blank), recorded in 78 study sites ordered from low to high and classified according the site type.

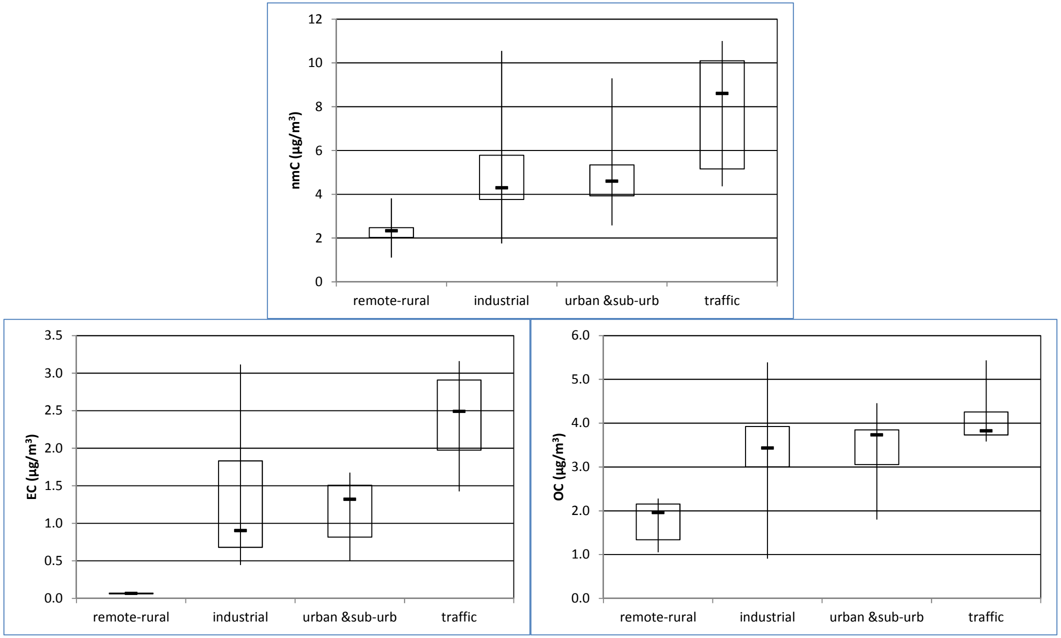

Fig. 3. Maximum, minimum, p25, mean and p75 values for nmC, EC and OC concentrations measured in this study.

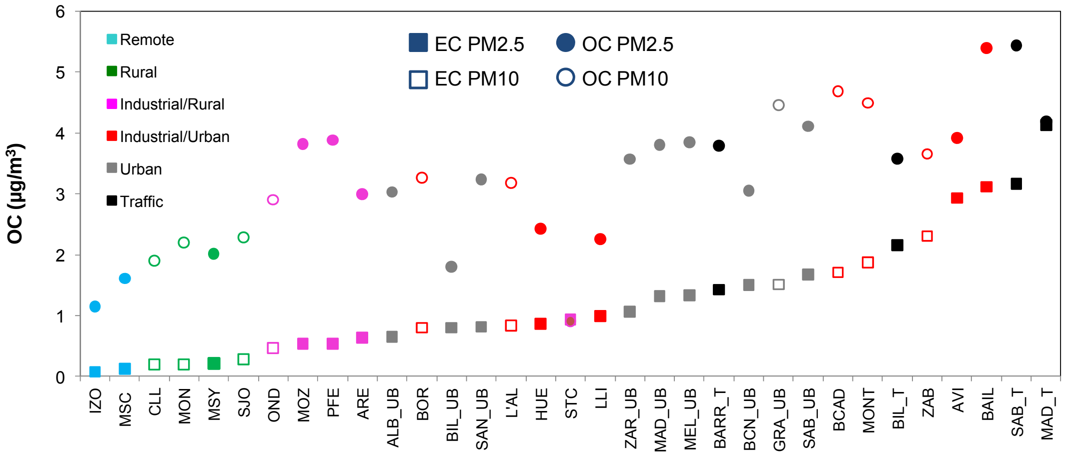

Fig. 4. Mean EC and OC levels in $PM_{2.5}$ (solid) and PM_{10} (blank) recorded in the 33 study sites ordered from low to high EC levels and classified according to the site type.

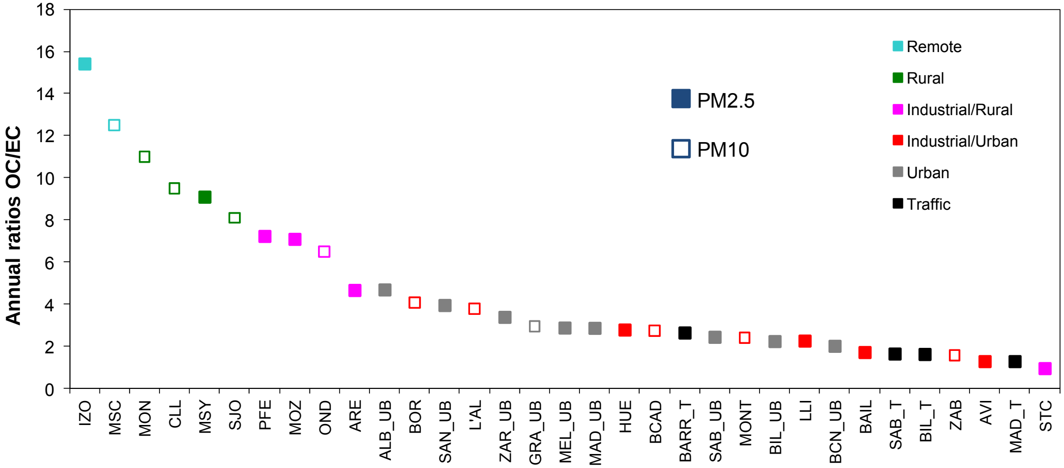

Fig. 5. Mean annual OC/EC ratios in $PM_{2.5}$ (solid) and PM_{10} (blank) recorded in the 33 study sites ordered from high to low and classified according to the site type.

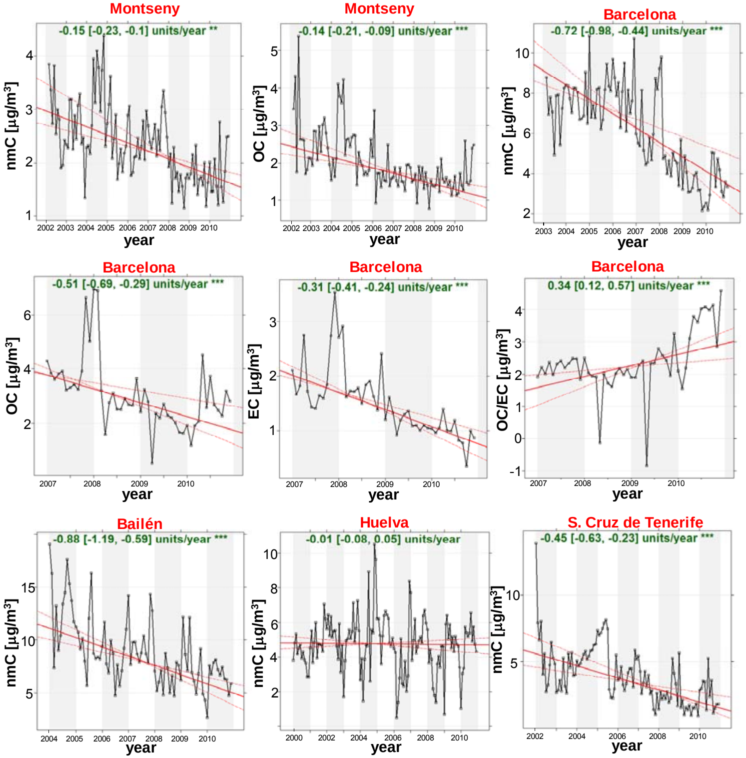

Fig. 6. Temporal trends for nmC in $PM_{2.5}$ at Montseny, Barcelona, Bailén, Huelva and Santa Cruz de Tenerife. The plots show the deseasonalised monthly mean concentrations. The solid red line shows the trend estimate and the dashed red lines show the 95 % confidence intervals for the trend. The overall trend and the 95 % confidence intervals in the slope (between brackets) are shown at the top as units ($\mu g\,m^{-3}$) per year. The ** and *** show that the trend are significant to the 0.01 and 0.001 levels, respectively. The OC concentrations for Montseny (2002–2010) and the OC and EC concentrations and OC/EC for Barcelona (2007–2010) are also presented.

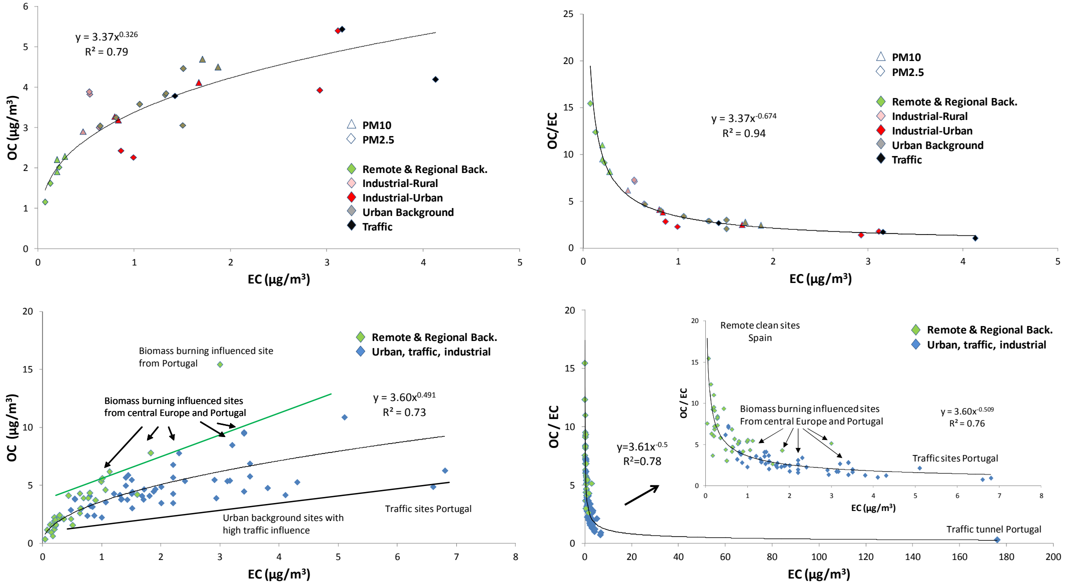

Fig. 7. Correlation and regression equations between mean OC and EC levels (two left) and the ratios OC/EC with EC levels (two right) obtained in this study for Spanish only (two top) and Spanish and other European (bottom) sites (Ytri et al., 2007; Pio et al., 2007, 2011; Grivas et al., 2012, and references therein).

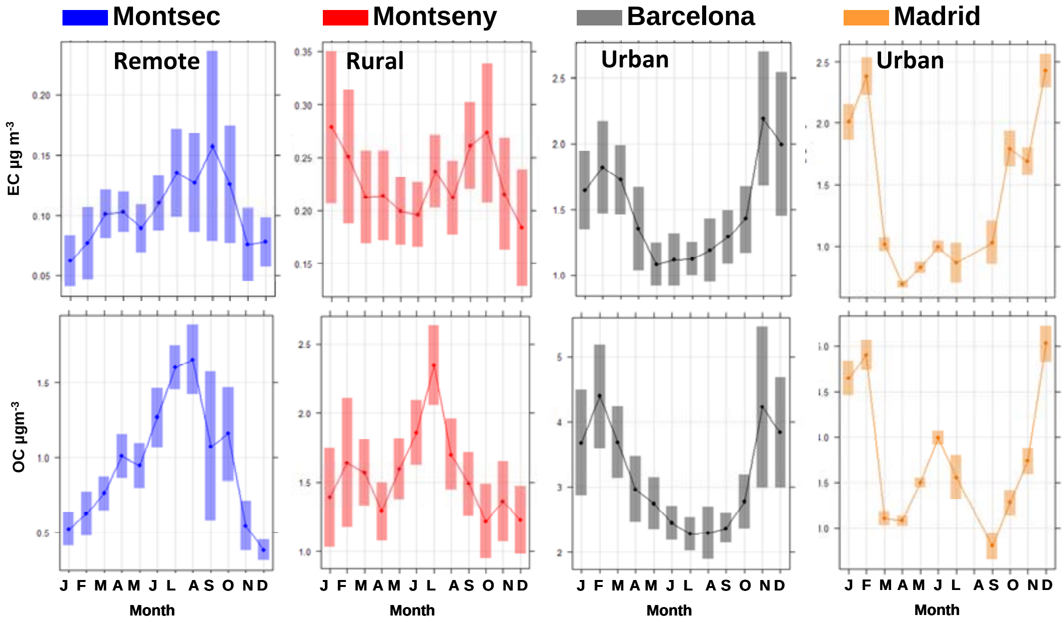

Fig. 8. Monthly mean OC and EC concentrations in $PM_{2.5}$ at Montsec (remote), Montseny (rural), Barcelona and Madrid (urban background and traffic sites). Bars represent 95 % confidence intervals.

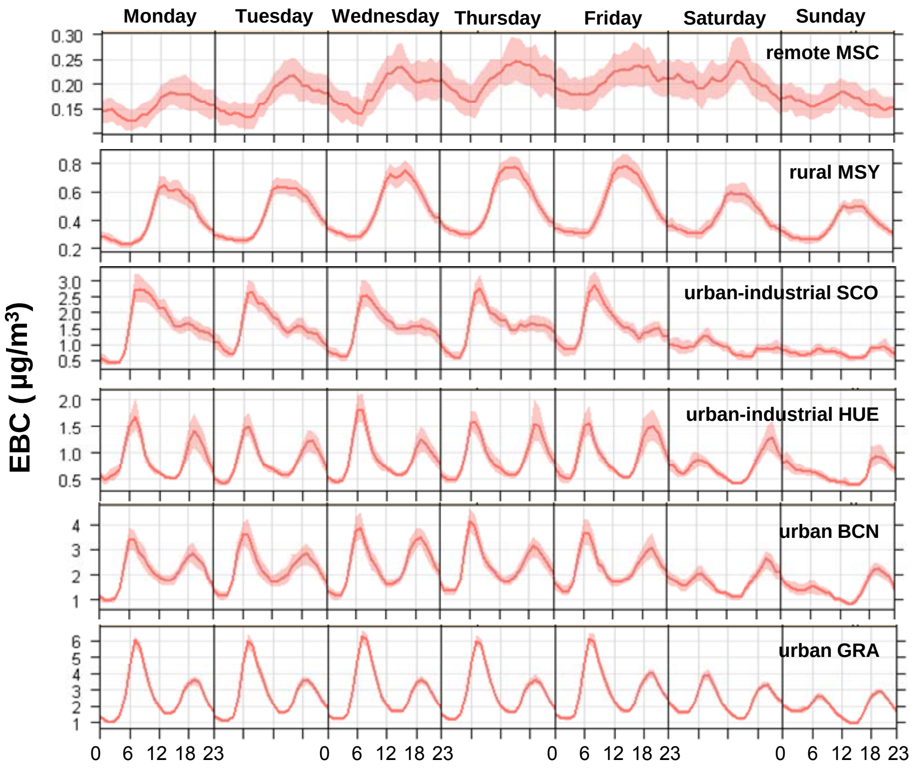

Fig. 9. Mean diurnal patterns of EBC at different environments in Spain. Shaded areas represent 95 % confidence interval in the mean.

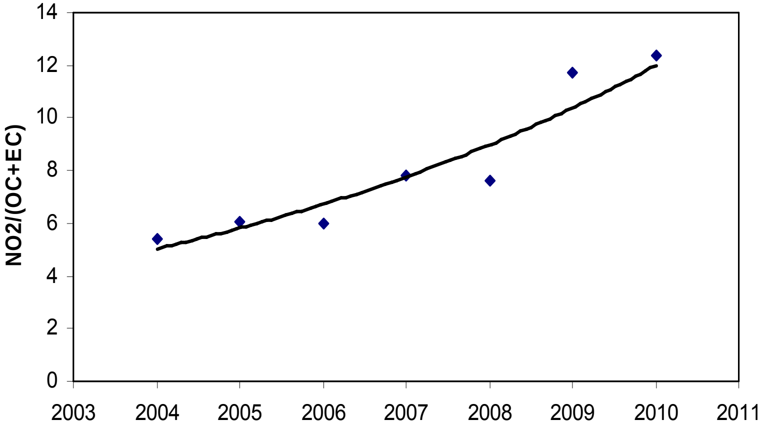

Fig. 10. $NO_2/(OC+EC)$ rates as obtained from OC + EC measurements in $PM_{2.5}$ performed at the Barcelona urban background site and from NO_2 measured at another urban background site in Barcelona (Ciutadella) by the Air Quality Department of the Autonomous Region of Catalonia.